FACULDADE DE ENGENHARIA DA UNIVERSIDADE DO PORTO

Hybrid DC Circuit Breakers for DC Grids

Antónia Teixeira Serra Belém Lima

FINAL VERSION

Master in Electrical and Computer Engineering

Supervisor: Professor António Pina Martins

October 9, 2023

Abstract

Wind power is part of the major renewable energy sources. Although the majority of the wind power plants are onshore, the number of wind power plants offshore has been increasing. The following dissertation presents the basic elements and functions of an offshore wind farm grid with a high voltage direct current (HVDC) transmission, wind energy conversion, wind turbines, transformers, reactive compensators, electronic power converters and DC circuit breakers (CBs).

The study and simulation of hybrid CBs (based on fast mechanical disconnectors and IGBT/diode modules) is the main focus of the dissertation, due to the challenges that result from HVDC transmission faults, and the fast response of this type of circuit breakers towards the faults mentioned. Hybrid CBs are compared with mechanical CBs and semiconductor based ones using several tests and clearly demonstrate their superior ability to be used in those grids.

Resumo

A energia eólica representa grande parte de recursos da energia renovável. Apesar da maioria das centrais eólicas serem em terra, o número de centrais eólicas instaladas no mar tem vindo a aumentar. A seguinte dissertação apresenta os elementos e funções de uma central eólica offshore com uma transmissão de alta tensão e corrente contínua, conversão de energia eólica, turbinas, transformadores, compensadores reativos, conversores de potência e disjuntores de corrente contínua.

Sendo o foco principal da dissertação o estudo e simulação de disjuntores híbridos de corrente contínua, devido a complicações que resultam de falhas em transmissões de alta tensão de corrente contínua, e a velocidade de resposta desse tipo de disjuntores às falhas mencionadas. Os disjuntores híbridos são comparados com disjuntores mecânicos e disjuntores baseados em semicondutores, através de diferentes testes, demonstrando a sua aptidão superior para ser utilizado nessas redes.

Acknowledgments

I would like to express my gratitude to my advisor, Prof. Dr. António Martins, for all the guidance and availability to help me during this last year. I would also like to thank my family and friends for all the support during my academic years.

Antónia Lima

Contents

List of Figures

List of Tables

Abbreviations and Symbols

Abbreviations list (in alphabetic order)	
AC	Alternating Current
B2B	Back to Back
CB	Circuit Breaker
DC	Direct Current
DCCB	DC Circuit Breaker
DFIG	Doubly Fed Induction Generator
FRC	Fully Rated Converter
GOOSE	Generic Object Oriented Substation Event
GSC	Grid Side Converter
HVAC	High Voltage Alternating Current
HVDC	High Voltage Direct Current
IEC	International Electrotechnical Commission
IED	Intelligent Electronic Device
LAN	Local Area Network
LCC	Line Commutated Converter
MOV	Metal-Oxide Varistor
MT-HVDC	Multiterminal High Voltage Direct Current
PCC	Point of Common Coupling
PWM	Pulse Width Modulation
RSC	Rotor Side Converter
RTU	Remote Terminal Unit
SAS	Substation Automation System
SCIG	Squirrel-Cage Induction Generator
SVC	Static Var Compensator
STATCOM	Static Synchronous Compensator
TCR	Thyristor Controlled Reactor
TSC	Thyristor Switched Capacitor
VSC	Voltage Source Converter
VI	Vacuum Interrupter
XPLE	Cross-linked polyethylene
Symbols list	
C_p	Coefficient power
v	Wind speed
ω	Rotational Speed
ρ	Air Density
λ	Tip-speed Ratio

Chapter 1

Introduction

The use of renewable energies reduces the emission of greenhouse gases, since the main cause is the energy production using fossil fuels, while renewable energies are clean. Utilizing renewable energy sources, which are unlimited, such as hydro, wave, wind and solar photovoltaic also decreases the necessity to import energy sources from other countries, allowing an energy independence, contributing to a better economy.

In Portugal, hydro energy was the first renewable energy implemented. However, in the last decades, wind energy was the most improved.

Wind power is part of the major renewable energy sources. Although the majority of the wind power plants are onshore, the number of wind power plants offshore has been increasing especially due to the less wind turbulence at sea, which allows higher wind speed and, in result, more power can be produced with a smaller number of wind turbines. However, there are no transmission and distribution systems offshore, so each wind farm is connected to shore with a high voltage AC link if the distance is less than 80 km [1]. Otherwise, it becomes more economic and effective to use a High-Voltage Direct Current (HVDC) interconnection.

Since wind farms are getting build further and further away from the coast, there is also the possibility of creating an offshore grid that combines all the wind farms of a certain area and brings the power produced to the land. This grid would also use HVDC technology. Due to the difficulty on maintenance offshore and the use of HVDC the electrical system must be extremely reliable, therefore, it needs to have a proper protection architecture. The main protection device is the circuit breaker (CB). Mechanical circuit breakers, semiconductor-based CB and hybrid CB are the main choices for implementing the protection in DC lines or grids. The dissertation focuses on the study of hybrid DC circuit breakers, which have a very low switching time, allowing a fast interruption of faulty currents and avoiding the damage of equipment.

1.1 Software Tools

In order to begin the test and analyse of the mechanical and hybrid DC CB there were two simulation software packages taken into consideration:

- MATLAB/Simulink – A model-based platform that supports system-level design, simulation, automatic code generation, and continuous test and verification of systems. Enables the incorporation of algorithms (from MATLAB) into models and export simulation results to MATLAB for further analysis;
- PSCAD – Used to build, simulate and model power systems. The data is managed in a completely integrated, graphical environment.

Either tools offer appropriate models to develop and test the hybrid circuit breaker performance in different conditions of operation.

Besides the most common elements like voltage source, passive elements and IGBT/diode models both offer different levels of complexity for DC cables/line models and surge arresters, required for a precise simulation modelling and reliable results. Due to availability and licensing, the MATLAB/Simulink/Simscape was chosen for developing this work.

1.2 Document Structure

The document is composed by four parts. Chapter 1, which is the present chapter and consists of an introduction to the dissertation's theme.

Chapter 2 is dedicated to the state of the art of offshore wind farms, including their electrical composition, AC and DC protection characteristics, and different types of HVDC circuit breakers.

Moreover, in chapter 3 models of mechanical DC circuit breakers and hybrid DC circuit breakers are implemented in different scenarios, as well as conclusions about the results obtained are presented and compared.

Finally, chapter 4 has a summary of the conclusions of the dissertation and offers future work perspectives.

Chapter 2

Background and State of the Art

2.1 Wind Energy Conversion

Wind turbines extract kinetic energy from the swept area of the blades and convert the wind power into the mechanical-rotational energy of the rotor of an electrical generator, resulting in a reduced speed in the air mass. Therefore, not all wind power can be extracted, as (2.1) presents, because the air mass would be interrupted in the intercepting rotor area [2]. Hence, the maximum power transferred to the wind turbine is constrained by the power coefficient (C_p), whose maximum value is the Betz limit. The Betz limit declares that only 59% of the wind power can be extracted by a wind turbine [1].

$$P_{(windturbine)} = \frac{1}{2}\rho A v^3 C_p(\lambda, \beta) \tag{2.1}$$

Where:

ρ – Is the air density (kg/m^3); A – Is the area where the air mass flows through (m^2); v – Is the wind speed (m/s); C_p – Power coefficient.

Furthermore, to determine the performance of any wind turbine rotor is also necessary to calculate the tip-speed ratio, λ (2.2), since the maximum power coefficient can only be achieved at a single tip-speed ratio [3].

$$\lambda = \frac{\omega R}{v} \tag{2.2}$$

Where:

ω - Is the rotational speed of the rotor; R – Is the radius of the blade.

The subsequent graphic demonstrates the variation of the wind power production with the wind speed, also known as the power curve of a wind turbine:

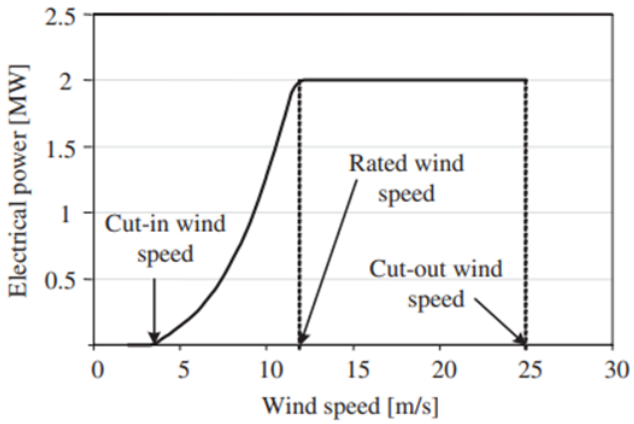

Figure 2.1: Typical 2 MW Wind turbine power curve [3]

The three velocity points shown in Figure 2.1 represent [2]:

- Cut-in wind speed – Is the velocity of wind at which the wind turbine will start to produce useful power;
- Rated wind speed – It can be between 12-16 m/s, depending on the design of the wind turbine. Is the velocity at which the maximum capacity of power production is reached;
- Cut-out wind speed – In the range of 20-25 m/s. When this velocity is exceeded the turbine stops working and producing energy. In addition, when the wind velocity finally drops below the cut-out wind speed, the turbines will only restart after a drop in wind speed of 3-4 m/s.

2.2 Offshore Wind

As it was shown previously, the key determinant of the wind potential at any given wind site is the average wind speed. Additionally, wind speed varies with location and wind turbulence [1]. An offshore site typically has less turbulence than onshore, because the sea surface is smoother and doesn't cause obstructions or interruptions to the wind flow, since there are no hills or mountains. These benefits result in more energy production with fewer wind turbines.

Although offshore wind turbines are very similar to onshore wind turbines, they are larger, their foundation must be built in the seabed and have to be more robust due to the corrosive nature of salt water. Consequently, the cost of construction and maintenance is higher [4].

However, gaining permission to build offshore is easier, due to the availability of large sea areas and less visual and noise impact.

2.3 Offshore Wind Turbines

Wind turbine generators can be divided into two categories, fixed-speed wind turbines, and variable-speed wind turbines.

Fixed-speed wind turbine employ a three-phase squirrel-cage induction generator (SCIG) powered by the turbine via a gearbox and directly connected to the grid through a step-up transformer, as the next figure shows:

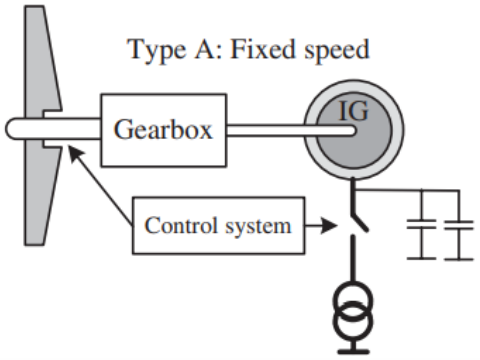

Figure 2.2: Fixed-speed wind turbine with induction generator [3]

As a result, the induction generator will provide an almost constant rotational speed. In addition, a capacitors bank is utilized, by the induction generator, for reactive power consumption. Nowadays, there are fixed-speed wind turbines equipped with capacitors that use power electronic switches for fast reactive power compensation control [3].

On the other hand, variable-speed wind turbines achieve the respective variable-speed either by controlling the rotor resistance of the induction generator, as shown in Figure 2.3, or by a power electronic frequency converter between the generator and the grid, which are the types of wind turbines used in offshore wind farms. One kind is the Doubly-Fed Induction Generator (DFIG), which has a converter rated about 30% of the generator, and the other is the Fully Rated Converter (FRC), that has a converter rated about 100% of the generator [3].

Furthermore, the converters mentioned above are voltage source converters (VSCs) since they allow the independent control of active and reactive power.

2.3.1 Doubly Fed Induction Generator

The Doubly Fed Induction Generator (DFIG) wind turbine has held the leading position as the primary variable-speed technology in the market for models exceeding 1.5 MW [3]. In this design, the stator windings are directly linked to the AC grid through the turbine transformer, while the rotor windings are connected to the AC grid through slip-rings and a back-to-back (B2B) power electronic converter, as demonstrated in Figure 2.4. The main components of a DFIG wind turbine are [3]:

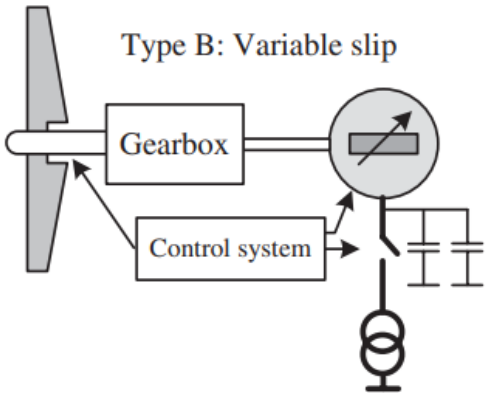

Figure 2.3: Variable-Speed wind turbine, with control of the induction generator rotor resistance [3]

- Induction Generator (IG);
- Back-to-Back Converter - Composed by two three-phase VSCs that are the rotor-side converter (RSC) and the grid-side converter (GSC), connected through a common DC bus;
- Gearbox – Responsible for stepping up the speed of the low-speed rotor to a higher speed suitable for the electrical generator;
- Crowbar Protection – During an AC grid fault, the crowbar disconnects the RSC and short-circuits the rotor windings to a bank of resistors, protecting the B2B from over currents.
- Modern crowbar protection circuits use power electronic devices such as IGBTs or GTOs;
- Turbine Transformer – Located typically at the base of the wind turbine tower.

2.3.2 Fully Rated Converter

This type of wind turbines, as shown in Figure 2.5, can come equipped with or without a gearbox, and they offer a wide array of electrical generator options, including asynchronous, conventional synchronous, and permanent magnet types. The power converter plays a crucial role in transferring all the power generated by the wind turbine, effectively isolating the specific characteristics and dynamics of the electrical generator from the power network. Consequently, allowing the electrical frequency of the generator to vary with changes in wind speed while keeping the network frequency constant, facilitating variable-speed operation. The Generator-Side Converter (GSC) can be either a diode-based rectifier or a PWM Voltage Source Converter, while the Network-Side Converter (NSC) is typically a PWM Voltage Source Converter. There must be some considerations taken into account with offshore wind turbines, such as [3]:

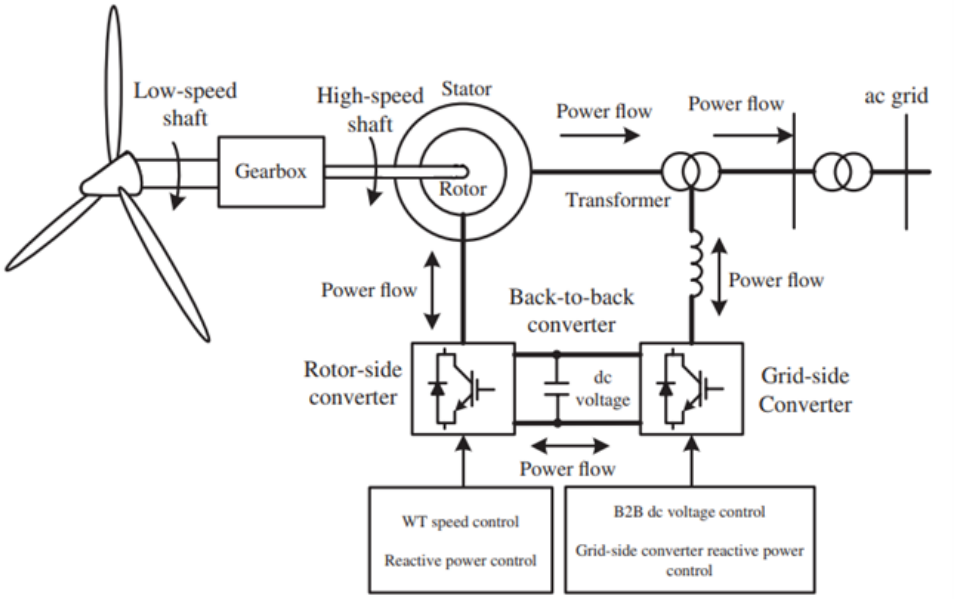

Figure 2.4: Diagram of a DFIG connected to a wind turbine [3]

- In order to maximise the potential of offshore wind energy, larger turbines with extended blades mounted on taller towers are commonly employed. This approach allows for greater efficiency and effectiveness compared to onshore designs;
- Offshore wind turbines must be highly robust and reliable, because they cannot be accessed at some times because of wind, waves and other weather conditions;
- There may be damage from sources such as:
  - Corrosion due to aggressive salty environment;
  - High wear due to heavy mechanical loads and higher utilisation;
  - Failures affecting gearbox, generator, transformer, blades and transmission cables;
- Size and capacity of offshore wind turbines have increased considerably;
- Unlike onshore sites, where wind turbine size is often constrained by restrictions on height and rotor diameter, offshore wind turbines have the advantage of operating in the open sea without encountering such limitations;
- Wind turbine components need to be pre-assembled onshore to allow quick installation offshore;
- From arrival at site the installation of a wind turbine takes a minimum of 24 hours;

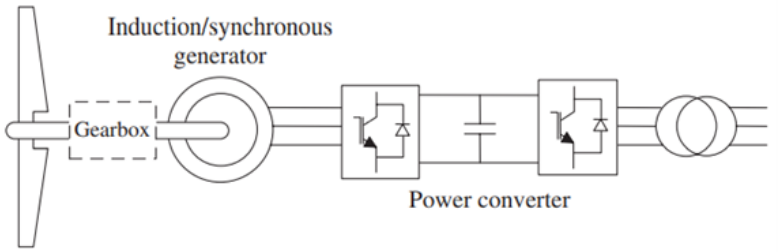

Figure 2.5: Configuration of a FRC (back-to-back) connected to a wind turbine [3]

2.4 AC Network

The offshore wind farms in study are composed of an AC side and a DC side, connected by voltage source converters. Figure 2.6 illustrates an example of that composition.

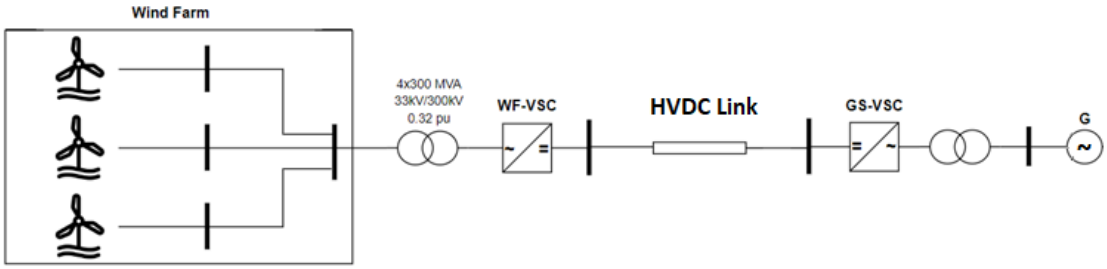

Figure 2.6: Wind farm connected to the grid (G) by a HVDC transmission link and a wind farm voltage source converter (WF-VSC) and a grid side voltage source converter (GS-VSC).

The AC wind farm network protection is divided into several protection zones, as Figure 2.7 demonstrates: wind generator protection zone, feeder protection zone, busbar protection zone and high voltage transformer protection zone.

The wind generator protections detect and isolate short circuits within the zone, however it may have backup protections. The feeder zone protection must be selective and only trip during faults within this zone or when operating as a backup protection for the wind generator protection zone. Furthermore, the busbar protection must also be selective and only be activated for a fault in this zone or if working as a backup protection for the feeder zone.

It is imperative to clear a busbar fault as fast as possible, due to the large currents' magnitude involved in this type of faults [3].

2.5 Transformers

As mentioned previously, the offshore power plants are located far away from the onshore grid, therefore, the voltage must be increased in order to transmit large volume of power through long distances. Hence, a transformer is utilized to achieve the increment of the output voltage.

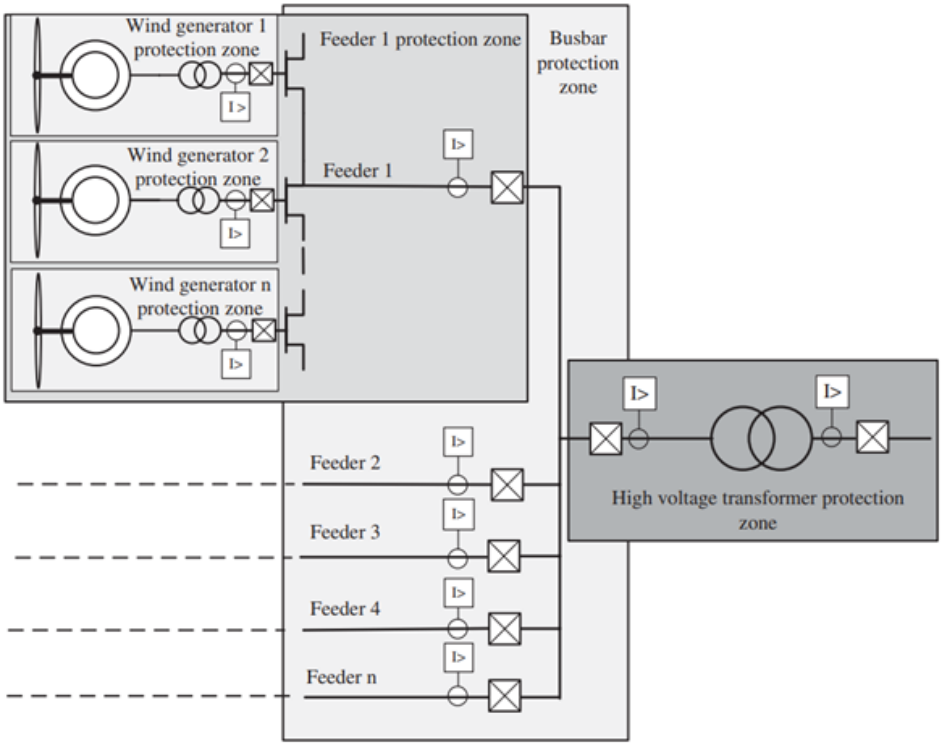

Figure 2.7: Protection Zones of a wind farm [3]

There are two varieties of transformers: power transformers, which are used for transmitting power over long distances at high voltages and distribution transformers, that distribute power to consumers at medium and low voltages. Furthermore, power transformers can be divided into more categories, such as generator step-up transformers, step-down transformers, HVDC converter transformer, phase shifting transformer, etc [5].

The type of transformer used in an offshore wind farm is the HVDC converter transformer, which connects the AC grid side to the high-power converter and elevates the voltage to a level suitable for the converter. Figure 2.6 shows that the transformer increases the internal AC grid voltage from 33 kV to 300 kV. In addition, this transformer also isolates the converter from faults in the AC grid [5].

2.6 Reactive Power Compensation

Large-scale wind farms have a great influence on the voltage stability of the main network [6]. In order to diminish this influence, the wind farm must have the capability of supplying reactive power to the power system, allowing the voltage control of the network.

There are two types of reactive compensation equipment utilized in these situations, Static Var Compensators (SVCs) and Static Synchronous Compensators (STATCOMs), which are variable static reactive power generators [5].

SVCs have the capacity to draw inductive or capacitive current from the network, requiring the existence of different designs of SVCs. The existing arrangements are a fixed capacitor with a thyristor-controlled reactor (TCR), Figure 2.8, and a thyristor-switched capacitor (TSC) with a TCR, Figure 2.9. The thyristors have the advantages of enabling a smooth control of the TCR and allowing the TSC to be a fast switched element [3]. However, the generation of low-frequency harmonics is a serious problem, turning this compensation type somewhat problematic.

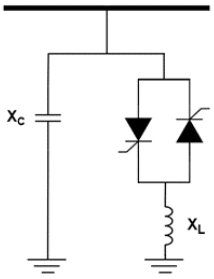

Figure 2.8: SVC with a fixed capacitor and a TCR

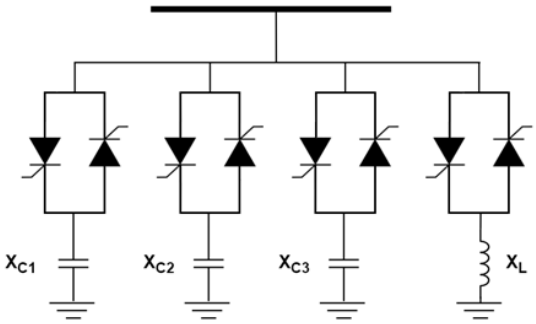

Figure 2.9: SVC with a TSC and a TCR

STATCOMs are VSC-based devices, with a large capacitor acting as voltage source. These equipment are composed of a two-level (or multilevel) VSC, a capacitor (to enable the storage of the DC energy), a coupling transformer (associated in shunt with the AC system) and the correspondent control systems [3], as Figure 2.10 shows.

Compared with the SVC, the STATCOM achieves faster response times, mainly because of its natural response to counteract the AC voltage amplitude, and also due to the switching frequency of the VSC. In addition, the reactive power from a STATCOM varies linearly with the AC voltage [3], allowing an improved reactive power support during low AC voltages, which with SVCs can only be reached if they are installed with a much larger capacity, making the STATCOM a more economic choice [6].

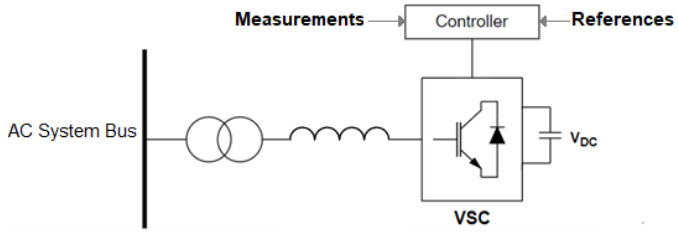

Figure 2.10: Basic configuration of a STATCOM.

2.7 Power Electronics Converters

The most suitable converters for a HVDC transmission system are the line commutated converter HVDC (LCC-HVDC), which is a thyristor-based converter, or the voltage source converter HVDC (VSC-HVDC), an IGBT-based converter Figure 2.11 and Figure 2.12 represent examples of these types of topologies, respectively.

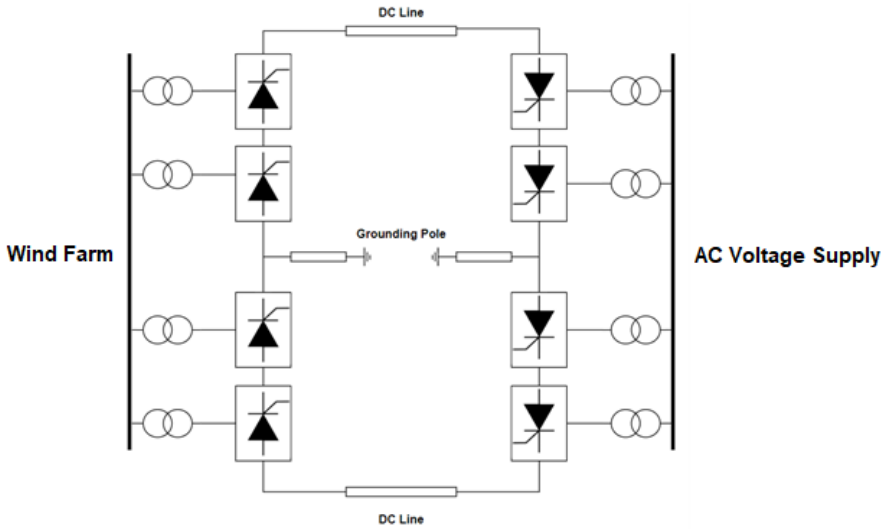

Figure 2.11: Typical LCC-HVDC system topology.

The normal operation of the thyristors of the LCC-HVDC requires voltage commutation and offshore wind farms have weak grids that cannot assure a strong voltage supply needed for reliable commutation. However, the use of fully-controlled IGBT switches of the VSC-HVDC avoids the commutation failure even in weak grids. The VSC-HVDC system presents even more advantages such as those highlighted in [4], [7], [8]:

- Independent control of the active and reactive power;
- The ability to operate as a STATCOM and provide reactive power to the AC system, increasing the voltage at the PCC;

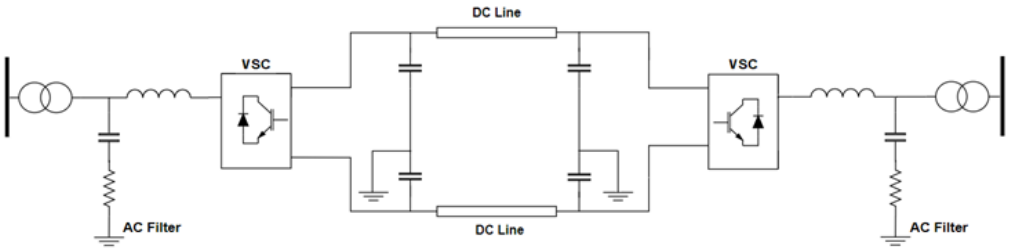

Figure 2.12: Typical VSC-HVDC system topology.

- Less harmonic distortion;
- Allowing the construction of a HVDC grid with many terminals (multiterminal grid).

Nevertheless, when a short-circuit occurs in a HVDC grid, the fault spreads faster and deeper in consequence of the low impedance of this type of grids. Furthermore, the voltage decreases, which can make the converters to lose control capability and, in result, lead to a voltage collapse and high currents. In order to prevent the previous effects, it is requested for the HVDC voltage to be at least 80 percent of the nominal HVDC voltage [8] and the fault to be cleared within 5 milliseconds (to not disrupt converter stations as far away as 200 km) [8].

Therefore, a VSC-HVDC system requires fast and reliable circuit breakers to isolate faults and avoid a collapse of the HVDC grid voltage.

2.8 DC Transmission Line Fault

A fault on the DC line discharges the DC capacitors of the VSC-HVDC (as shown in Figure 2.13) and, consequently, the converter station is incapable of interrupting the feeding of the fault current coming from the AC side through the diodes (the IGBT's are blocked).

The interruption of a DC current in a VSC-HVDC link can't be done by AC CBs, because, under these conditions, they will generate an arc capable of burning the switchgear, or due to the time period of the process of opening and closing the AC CBs, that can take up to 2 seconds, in circumstances where a great amount of power is transmitted it affects the AC network stability.

Another concern during this type of fault is the induced transient currents circulating through the valves of the VSC-HVDC station and to protect the anti-parallel diodes of the IGBTs the interruption of the DC current must be executed in the order of milliseconds.

The fault pole-to-pole, illustrated in 2.13, is the most serious fault that can take place in the DC side of the VSC-HVDC network. Some simulation studies have shown the magnitude of the initial fault current for a pole-to-pole fault can be up to 73 times the nominal DC current [3]. Hence, it is required to use DC CBs, since they have a short period of interruption and, therefore, can avoid the permanent damaging of the IGBTs' diodes.

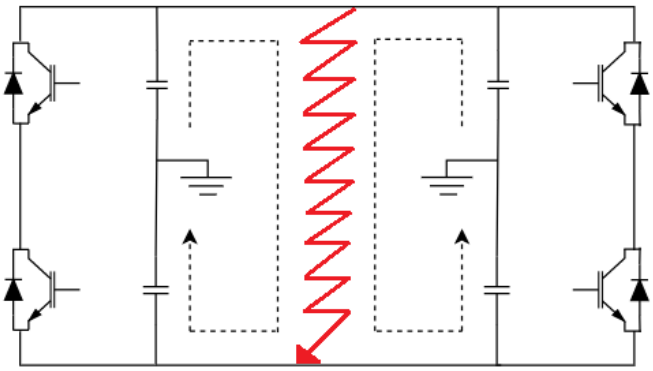

Figure 2.13: DC pole-to-pole fault in a transmission line/cable.

2.9 HVDC Networks

In order to break HVDC currents, a DC breaker is frequently placed between the converter and the DC line. The rate of a current rise could be extremely high during a fault, due to the impedance on the DC side that is significantly small. Therefore, a DC inductor is typically positioned in series with the breaker [9]. In addition, all high-power AC/DC converters have self-protection control logic, which consists of blocking and disconnecting the converters in the event of disturbances [10]. However, the circuit breaker location can differ according to the grid topologies.

HVDC transmissions are mainly point-to-point links between two AC systems, as shown in Figure 2.14. Nevertheless, with the development of HVDC transmission systems, future HVDC grids will involve existing HVDC links connected to each other, reducing the cable length and number of converter stations, resulting in multi-terminal HVDC networks, as Figure 2.15 represents [11], [12].

Figure 2.14: Potential North Sea offshore wind point-to-point connection [12]

In a point-to-point HVDC system adequate protections for DC faults are simple, because selectivity is not an issue, as a result, HVDC circuit brakers are not necessary [12], [13]. On the other

Figure 2.15: Potential North Sea offshore wind multi-terminal connection [12]

hand, the problem is much more difficult for complex DC grid topologies such as multi-terminal HVDC grids.

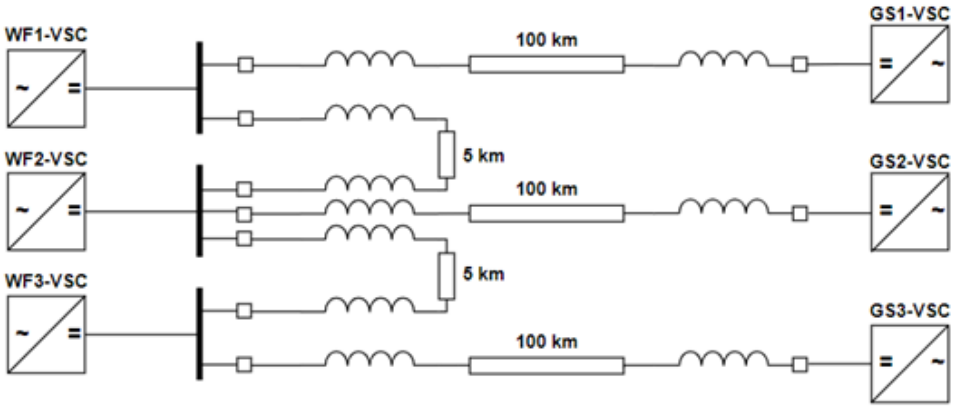

Figure 2.16: Multi-terminal HVDC wind farm., adapted from [12]

Figure 2.16 characterizes the example of Figure 2.15, a multi-terminal HVDC wind farm, three different blocks of a wind farm are connected to shore via HVDC links utilizing 100 km long XLPE cables. The offshore converter stations are then connected on the DC side using shorter cables. DC cable fault protection is achieved with the placement of DC circuit breakers at the ends of each cable, alongside inductors to facilitate fault discrimination and limit the fault current [12].

The distribution of the DCCBs along the transmission lines ensures that in the event of a permanent DC fault on a line, that faulted line will be immediately selectively disconnected and system's stability will be re-established [14].

2.10 Circuit Breakers

Circuit breakers are switching devices that usually remain closed and act as electrical conductors, but besides being capable of carrying current, they can also break currents in order to protect the grid from abnormal circuit conditions such as short circuits and other circuit faults.

To assure the protection of every type of grid there are different parameters and characteristics for circuit breakers, for instance [15]:

- Intended voltage application – Circuit breakers can be used in low, medium and high voltage grids, however, they must be rated (maximum voltage or current) according to the grid and possible fault parameters;
- Installation – Depending if a circuit breaker is installed indoors or outdoors, the design will differ;
- Medium used for current interruption – the circuit breaker technology depends of the interruption medium, being sulfurhexafluoride (SF6) and vacuum the most utilized, but air and oil are also used.

The two essential functions of a circuit breaker are to open and close their contacts on command. The separation of CB contacts under a current flow creates an arc, which in high-voltage systems generates large amounts of heat caused by the arc resistance [10]. The electrical arc is a physical phenomenon created by the dissipation of energy in an electro-mechanical switching device. In order to prevent the phenomenon mentioned the switching device has to dissipate the energy in the circuit, before the interruption of the current, bring the current to a zero value and then it must provide a dielectric barrier to prevent the restarting of the current flow [16].

In AC circuits the instantaneous value of the current passes through zero twice during each cycle and the contacts open during the zero-crossing, which contributes to a minimum dissipation of energy. Any energy in the system is conveniently dissipated in an arc chamber [10].

In contrast, DC systems do not have natural current-zero crossings, therefore a current-zero has to be forced. The forcing of a current zero is done either by increasing the arc voltage to a level that is equal, or higher than the system voltage, or by injecting into the circuit a voltage with an opposite polarity to that of the arc voltage, which is the correspondent of forcing a reverse current flowing into the source, through the usage of power electronic devices such as solid state devices (i.e. IGBTs) or a LC resonant circuit. [15], [16], [17].

2.11 DC Circuit Breakers Challenges

As mentioned previously, the faulted line needs to be isolated as fast as possible, otherwise the grid voltage will decrease, which reduces the power transferred, and the currents will increase, and consequently damage electrical components.

Current investigations are focusing on the research and development of solid-state DC breakers (IGBT based) where the switching time can be as low as a few microseconds [18].

Moreover, HVDC grid system performance is not the only reason fast HVDC switches are necessary. From the point of view of HVDC breaker design, fast fault current breaking is also crucial. In systems of high voltage, the tripping of CBs creates a dangerous arc that, if not interrupted before reaching a certain temperature, can damage the electrical equipment. Another challenge

with the opening of DC CBs is the energy dissipation that, unlike with AC CBs, can be large in cases of high voltage. To counter this dissipation, DC CB's have resistors, also known as energy absorbers or surge arresters, integrated. This has implications in terms of cost, size, weight, and operating speed. Figure 2.17 represents a simplified equivalent HVDC circuit during an occurrence of a fault where Vdc represents the DC output of the HVDC station (i.e. a capacitor) and Ldc is an inductance ,sized according to specific protection requirements.

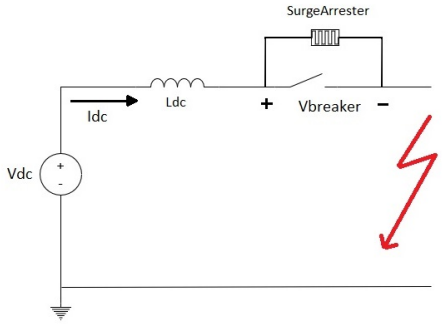

Figure 2.17: Simplified equivalent HVDC circuit during an occurrence of a fault.

The total time of fault clearing involves two parts: breaking times, which corresponds to a period of rising current, and fault clearing time, which consists of a period of decreasing current. The increasing and decreasing of current during the fault clearing of the example given in Figure 2.17 can be visualized in Figure 2.18.

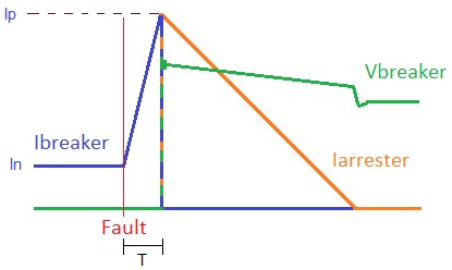

Figure 2.18: Current flow during a fault clearance.

The size of the inductor L_{DC} is related to the peak current (I_p) that occurs after the fault, the period (T) of the opening of the breaker (which is the period where the current is rising from its nominal value (I_n) to its peak) and the source voltage, as (2.3) describes.

$$L_{DC} = \frac{V_{DC}T}{I_p - I_n} \tag{2.3}$$

In addition, the surge arrester clipping voltage is commonly, in HVDC circuit breakers, 50% over the system voltage [18].

2.11.1 HVDC CBs Components

In order to build a HVDC circuit breaker, the following components have to be taken into consideration [13]:

- Mechanical switch – since the opening of the mechanical switch has a significant influence in the breaker isolation time, to assure the efficiency of the CBs they must be composed of a robust mechanical switch with excellent dielectric properties. To achieve that, the following characteristics have to be discussed:
  - Ultra-fast actuators - Magnetic repulsion based actuation mechanisms have been the main research. As alternative hydraulic actuators have been implemented in practical HVDC breakers.
  - Switching media – Vacuum Interrupter (VI) and Sulphur Hexafluoride (SF6) have superior dielectric properties in comparison with air-blast and oil HVDC breakers. VIs exhibit high dielectric strength while SF6 switches possess superior post-arc insulation strength. It has also been suggested the use of series of both switches combined.
- Inductor – It is usual to place an inductor in series with the DC circuit breaker because it limits the rate of rise of the current fault, which permits a longer time for the DC circuit breaker to clear the fault. However, the current limiting inductor causes conduction losses and also creates control challenges in the DC grid.
- Load commutation switch - The load commutation switch is used to transfer current from the normal conduction path to the main breaker. It must have low losses, a fast switching speed and high reliability. For these reasons, the IGBT is often used. A diode is added to the IGBT, in anti-parallel, allowing current conduction in the reverse direction and protecting the IGBT against reverse overvoltage.
- Main semiconductor breaker – It must carry and break full fault current. It is made of series of devices, and if necessary parallel devices, which makes the main breaker modularized. This allows the voltage to be adjusted when needed.
- Overvoltage protection - Most DC breaker designs rely on metal oxide varistors (MOVs), also known as surge arrestors, to limit over-voltages and dissipate the associated energy. Is composed of several columns of discs that are connected in parallel inside the same porcelain element. The energy absorbed must be rapidly dissipated, to avoid failure or degradation of the surge arrestor.
- Instrumentation, sensors, and communication - Must also be considered for indication of faulty components, and the need for potential remote operation.

2.11.2 Protection Relays

In order to instruct the circuit breakers to open or close, it is necessary to detect and locate the fault, which can be achieved without communication (only via local measurements) or by utilizing signals communicated from other terminals as well as the local measurements.

Regarding construction, protective relays can be broadly categorized as follows [19]:

Electromechanical Relays: These relays are designed for single functions but are no longer in common use.

Static Relays: This term is somewhat general and doesn't specifically define the internal circuitry of the relay for its intended functionality. Even electromechanical relays may incorporate static components, such as varistors in differential relays. In contrast, a static relay may consist entirely of solid-state components.

Digital Relays: The presence of digital technology characterizes these relays. They may include solid-state components like integrated chips, transistors, or other digital devices.

Numerical Relays: Typically based on microprocessors, numerical relays offer multifunctionality. For instance, a numerical relay can serve equally well in providing differential protection for transformers, generators, or motors.

Microprocessor-Based Multifunction Relays: These relays are currently the most popular choice and are employed in nearly all power system relaying applications. The era of discrete electromechanical relays, single-function relays, static relays, and digital relays has passed. The industry now demands protective relays capable of hosting numerous programmable protective functions, as well as offering control, metering, programmable inputs and outputs, pre- and post-fault data capture, and a wide array of communication protocols. These relays also feature self-diagnostic capabilities for both software and hardware failures.

The main protection techniques used in AC systems are [16], [19]:

- Overcurrent protections - A trip signal is sent to the CB, by an overcurrent relay, when the current surpasses a predefined threshold Overcurrent relays find extensive application in safeguarding both transmission and distribution networks. However, the growing adoption of distributed generation within distribution networks presents a challenge for conventional relays. This challenge arises from the variable short-circuit levels and load profiles in such systems. An adaptive approach involves analyzing these variations through an equivalent Thevenin circuit, which adapts to both fault and normal operating conditions. This circuit's alterations have an impact on the characteristics of time-overcurrent relays, specifically affecting trip times and pickup parameters. To address this issue, distance protection offers a viable solution.

- Distance Protections – Their duty is to measure the distance to the fault by analysing the apparent impedance, the ratio between the voltage and the current.

- Differential protection – Is responsible for measuring and comparing currents at the line ends. Differential protection relies on the fundamental concept that the current entering

a protected zone should be equal to the current leaving that same zone. This equilibrium in current flow is disrupted when a fault occurs within the protected area. These relays can be categorized into three types: Differential Overcurrent Relay, Percentage restrained differential relay and High impedance differential relay.

The protection systems mentioned previously (with the exception of differential protection) are not suitable for HVDC lines, mainly because they do not guarantee selectivity and have a large delay for this type of lines. Moreover, the following protections systems were proposed for DC lines [16]:

- Current and voltage derivative protections – Current derivative protections send a trip order when the current derivative exceeds a specific limit. A voltage derivative protection sends a trip signal when the voltage derivative is lower than a particular value;
- Travelling wave protection - Its algorithm is focused on the measurement of the magnitude and polarity of the current waves (or the voltage waves), initiated by faults.
- Artificial intelligence - Based on artificial intelligence techniques, for instance, machine learning.
- Differential protections – It is necessary to adjust the basic differential current principle. The modification takes into consideration the transient behaviour of a DC grid under fault conditions.

Additionally, there is the possibility of using a multipurpose Intelligent Electronic Device (IED), which has been used to monitor and control power networks, to experiment the different methods with different system configurations and different fault current interruption techniques, which will guarantee a compatible protection method to every HVDC line [16].

2.11.3 IEC 61850

To guarantee the fast response and reliability of a HVDC circuit breaker it is necessary to have a fast, reliable and real-time communication channel with the substation responsible for the power system.

Earlier the control of substations was based on discrete electronic or electromechanical elements, and several functions were carried out separately by specific subsystems. The microprocessor-based substation control systems were originally conceived as remote terminal unit (RTU)- centric architecture, and later on as local area network (LAN) architecture [20]. Nowadays, there is the concept of Digital Substation, which is a term applied to electrical substations where operation is managed between distributed intelligent electronic devices (IEDs) interconnected by communication networks [19].

IEDs are protective and control devices such as relays, circuit breaker controller, voltage regulators, etc. These devices are capable of accepting various levels of current and voltage inputs, and,

also, they are able to analyse those values at increased speeds. Additionally, IEDs can perform more than one function [19].

The development of the IEDs along with the implementation of the communication protocol IEC 61850 allowed the evolution of substation automation system (SAS).

IEC 61850 is a standard used in intelligent networks that represents the key component for the SAS, as well as protecting the transmissions within the network [21].

The main goal of this communication protocol is to assure a more flexible communication system for control, fast operation and high accuracy measurements in order to allow interoperability between different manufacturers [22].

Timing in the operation of the electrical SAS is extremely important and the IEC 61850 standard has the ability to deliver fast response information by using Generic Object Oriented Substation Event (GOOSE) protocol. This protocol supports the exchange of a wide range of possible common data that is organized by a DATA-SET, such as in synchronized circuit breaker switching, distance protection and overcurrent protection [21].

Moreover, the GOOSE is the light important function in IEC 61850 protocol to represent a status function from the remote IEDs to operate in the local IEDs. GOOSE messages are used to replace the hardwired control signal exchange between IEDs for interlocking, protection purpose, and sensitive missions that are time critical and require high reliability. IEC 61850 GOOSE message transmits a set of information that is "published", based on any changes in IED information. The message takes 4 ms, from occurring fault position to the trip operation, to take the necessary action to correct the fault and protect the substation from shutdown [20], [21]. Some examples of messages are the following [22]:

- Time-critical data such as trips, blocks, and interlocks.
- The data transfer initiated only on the occurrence of an event, for example, a trip, closing or opening of a breaker, and change in the status of an arc-flash maintenance mode switch.
- Data can be sent periodically for self-test and reliability.
- It is user defined: set of data that are "published" on the detection of a change in any of the contained data items.

These characteristics of IEC 61850 can significantly reduce costs associated with designing, installing, commissioning and operating power systems. Furthermore IEC 61850 uses an Ethernet connection as the physical medium of communication between IEDs. The implementations are able to send messages between protective relays at a speed of 1–4 ms. If IEDs and Ethernet connections are used, the blocking signal from the feeder IEDs to the main breaker IED can be transmitted fast, which will further reduce the arc-flash incident energy release.

2.11.4 DC CBs Topologies

There are three different topologies of DC CBs indicated for HVDC systems [8], [23]:

- Mechanical DC CB - Capable of conducting large currents with small losses. However, a fault current interruption takes several tens of milliseconds, which is too slow to fulfil the requirements of a reliable HVDC grid;
- Semiconductor-based DC CBs – Faster operation than mechanical CBs, but generate large power losses;
- Hybrid DC CBs – Even faster operation than semiconductor-based DC CBs, without significant losses.

2.11.4.1 Mechanical DC CB

The Mechanical DC CB has the following components, as seen in Figure 2.19:

- The main CB (Main) is usually closed, and it is rated for the full DC voltage of the DC voltage source (V_{DC}) and peak interrupting current;
- The residual breaker (Res) is similar to the main CB, however the requirements for opening speed and interrupting current are lower;
- The auxiliary CB (Aux) is normally open, has a similar rating to the main CB and a synchronised closing speed with the main CB opening speed.
- The surge arrester (SurgeArrester) dissipates the energy stored in the DC system preventing overvoltage;
- The L_r and C_r are responsible for generating AC current when the auxiliary CB is closed. Additionally, the charging resistor R_r enables the charging of C_r to rated voltage;

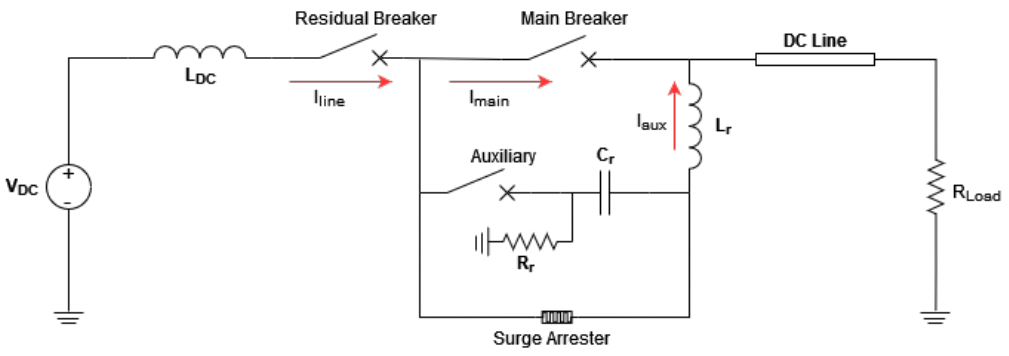

Figure 2.19: Mechanical DC circuit breaker.

After the trip signal is received, the main CB contacts start to separate, resulting in the formation of a DC current arc which cannot be extinguished solely by the CB. Moreover, the auxiliary CB is closed when the main CB is completely open.

The pre-charged C_r creates an oscillating LC circuit through L_r and an arc path in the main CB, which originates an AC current. This AC current is added to the DC current and creates a zero crossing in the main CB, interrupting the arc.

$$I_{main} = I_{line} - I_{aux} \tag{2.4}$$

The resonant circuit has to generate a current pulse equal to the DC breaker current, as given by (2.5). However, to ensure the interrupter succeeds is common that the prospective current magnitude exceeds this by some margin, which creates multiple zero crossings in case it was not successful at the first time.

Moreover, the frequency in (2.6) should be high to decrease the cost and volume of the resonant circuit's components. Nevertheless, a large frequency can make it challenging to interrupt successfully upon a current zero [24]. In practical devices this frequency is in the range 2–3 kHz [18]. Furthermore, defining the frequency of the oscillating current also defines the opening time of the auxiliary breaker, which is equivalent to the inverse of the frequency (2.7).

$$I_{line} = V_c(0)\sqrt{\frac{C_r}{L_r}} \tag{2.5}$$

$$f = \frac{1}{2\pi\sqrt{C_r L_r}} \tag{2.6}$$

$$t_{open} = \frac{1}{f} \tag{2.7}$$

As soon as the main CB current is interrupted, there is still a large DC current in the L_{DC}, that is discharged in the surge arrester. Furthermore, the residual CB interrupts leakage current through the surge arrester.

2.11.4.2 Semiconductor-based DC CB

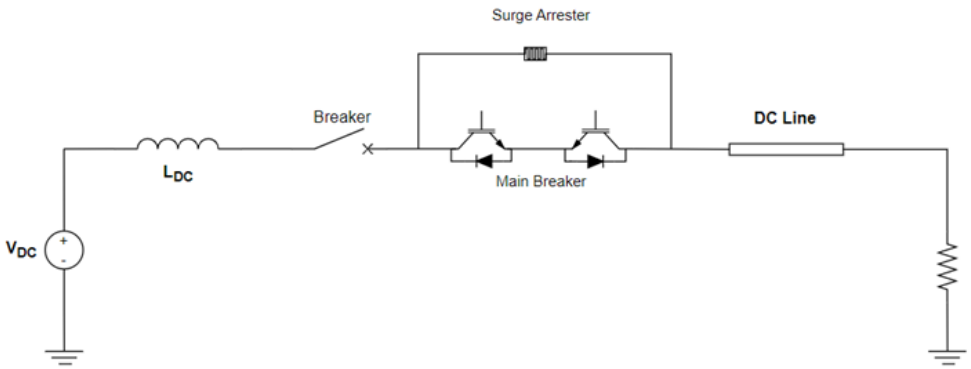

Figure 2.20: Bidirectional Semiconductor-based DC circuit breaker.

In addition, the semiconductor-based CB, Figure 2.20 can interrupt current in both directions and is composed of the subsequent elements:

- IGBTs with integral anti-parallel diodes, with valves with full DC voltage rating;
- The inductor Ldc, responsible for limiting the fault current derivative.
- A surge arrester, which releases all the fault energy in the DC circuit.

Semiconductor-based DC CBs are able to interrupt DC fault current much faster than mechanical DC CBs without requiring a current zero crossing. To interrupt the fault current hundreds of semiconductor switches (for instance IGBTs) are required. Additionally, to dissipate a large amount of energy, IGBT switches should be connected either in series and/or parallel, which results in high-total cost and power losses. The static and dynamic voltage sharing between individual IGBTs of CB HV valves is another issue, which adds to its complexity [25].

2.11.4.3 Hybrid DC CB

Furthermore, hybrid HVDC CB is composed by the main breaker and an auxiliary branch, as Figure 2.21 displays.

The extra branch consists of a fast mechanical disconnector in series with a semiconductor-based switch. Furthermore, the main breaker is semiconductor-based and constituted of separated sections, each with individual arrester banks dimensioned for full voltage and current breaking capability. The most suitable semiconductor is the IGBT, especially because: it is driven by voltage, allowing it to need less power, it is short-circuit-proof and has overloaded capability within its thermal capacity limit [23].

Additionally, after fault clearance, the residual current is interrupted, and the faulty line is isolated by a disconnecting CB. This action ensures the protection of the bank arresters from thermal overload.

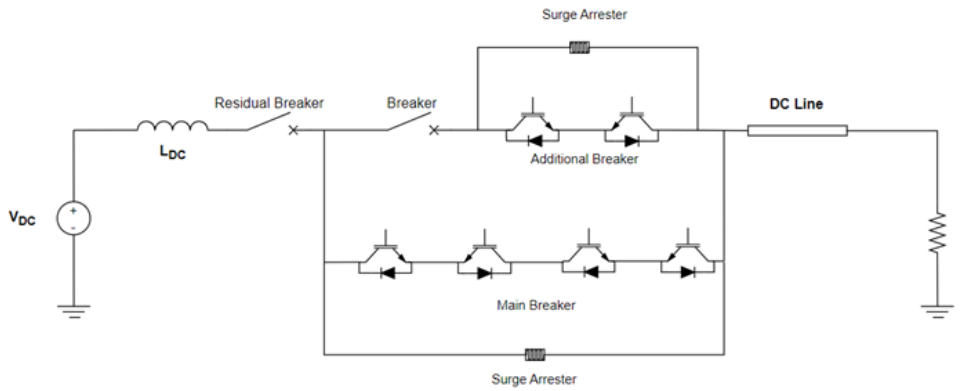

Figure 2.21: Hybrid DC circuit breaker.

During normal operation, with the two branches in on-state, the main current flows through the additional branch, while the current in the main breaker is almost zero. This is due to the fact that in the additional/auxiliary branch only one or two IGBTs conduct in series with a small voltage drop while the main branch contains hundreds of IGBTs in series. Thus, in the two parallel paths the current flows essentially through the auxiliary branch. If a HVDC fault occurs, the load commutation switch immediately commutates the current to the main HVDC breaker and the mechanical fast disconnector opens, allowing the main HVDC breaker to break the current, and isolating the load commutation switch from the primary voltage of the main breaker. Therefore, the required voltage is significantly reduced.

Proactive control of the hybrid HVDC breaker allows it to compensate for the time delay of the fast disconnector.

The main HVDC breaker is responsible for delaying current breaking until a trip signal of the protection system is received or if the faulty line current is reaching the maximum breaking current capability. Moreover, it is also accountable for the voltage drop across the HVDC reactor in order to prevent a further rise in the line current. The maximum duration of the current limiting mode depends on the energy dissipation capability of the arrester banks [8].

2.12 Discussion

There is an increasing need for formation of multiterminal HVDC (MT-HVDC) grids, due to the growth of large offshore wind farms at farther distances from the coast, and the VSC is considered the key technology for the development of the MT-HVDC grids.

Although the typical Hybrid CB has many advantages in terms of current interruption time and power losses, it requires hundreds of semiconductor switches in its main breaker (MB) branch to tolerate the system voltage. Consequently, its implementation cost is expected to be high.

A MT-HVDC grid will be composed of large wind farms located in different geographical areas connected through several submarine HVDC cables. Hence, a considerable number of Hybrid CBs might be required to have a fully selective protected MT-HVDC grid [26].

Chapter 3

Simulation Studies

3.1 Models

Before the implementation of the intended circuit in MATLAB/Simulink, some research was made to decide the parameters that should be utilized in the simulation in order to create a close to reality simulation.

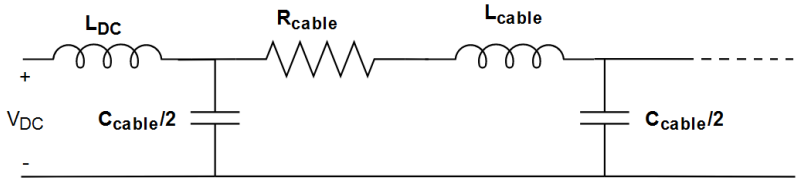

Figure 3.1: DC side model with the respective smoothing reactors and DC cable.

Figure 3.1 represents the DC cable and its parameters that will have to be introduced in MATLAB/Simulink. The following image shows the already existing values for each parameter of cables or lines, depending on their voltage: Due to the relatively high capacitance of cables as

Line data R	R (Ω km^{-1})	L (mH km^{-1})	C (μF km^{-1})
DC OHL $\pm$ 400 kV	0.0114	0.9356	0.0123
DC OHL $\pm$ 200 kV	0.0133	0.8273	0.0139
DC cable $\pm$ 400 kV	0.0095	2.1120	0.1906
DC cable $\pm$ 200 kV	0.0095	2.1110	0.2104

Figure 3.2: DC side model with the respective smoothing reactors and DC cable [18].

compared with overhead lines, the current to be interrupted is higher. In addition, the series inductance of a cable is nearly three times higher and the capacitance to earth is 20 times larger than those of an overhead line [27].

Moreover, the higher capacitance of a cable also has consequences for the system resonance frequencies, which are considerably lower. The distributed parameters nature of the (long) cable means a frequency response that depends on the distance where the fault occurs. And this will influence either the magnitude and the frequency of the voltage oscillations when a fault is cleared as will be shown in the results. In Figure 3.3 it is shown the frequency response of the cable described before for three distances between the VSC station and the fault location: 10, 30 and 70 km. As can be seen, the shorter the distance the higher the resonant frequency and the impedance.

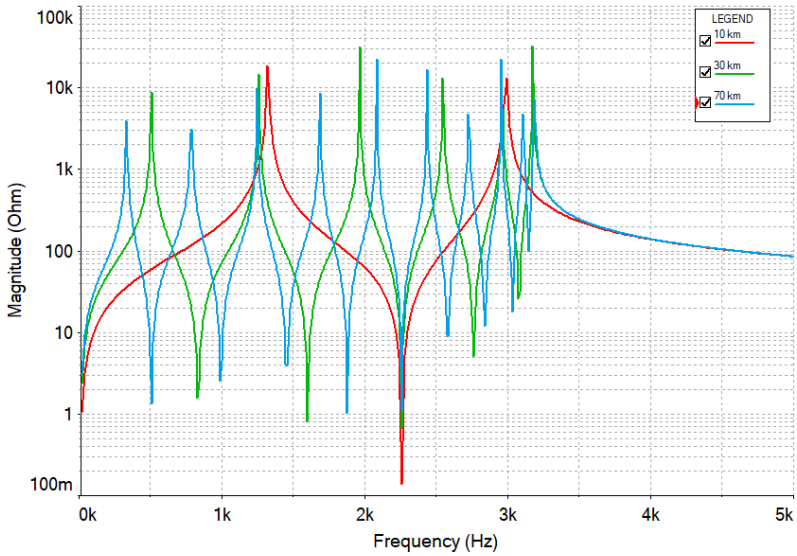

Figure 3.3: Cable's frequency responses.

Additionally, after encountering the most appropriate IGBTs from different manufacturers, as Table 3.1 presents, it was considered a single switch IGBT module (FZ 1800 R45 HL4, from Infineon) that has a capacity of 4500 V and 1800 A, enabling 1.4 GW HVDC Plants at +-320 kV without paralleling.

Table 3.1: IGBTs characteristics: Collector-emitter voltage (V_{CES}), Continuous collector current (I_C) and Peak collector current ($I_{C(peak)}$).

Manufacturer	A	B
Model	FZ1800R45HL4	DIM1200ASM45-TS000
V_{CES} (V)	4500	4500
Ic (A)	1800	1200
$I_{C(peak)}$ (A)	3600	2400

The diagram in Figure 3.4 was created and simulated in MATLAB/Simulink:

To simulate the residual and the fast-mechanical breakers it is utilized an ideal switch from the MATLAB/Simulink library that can be used as a circuit breaker with a current chopping.

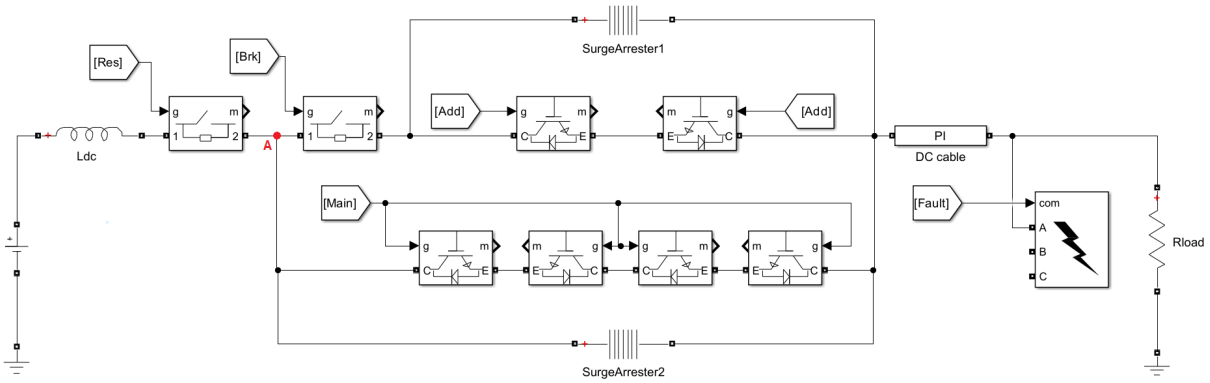

Figure 3.4: Hybrid CB built using MATLAB/Simulink.

The switch is controlled by the gate, when a positive signal is at the gate input (g>0) the switch is on and it turns off when the input signal equals 0 (g=0). Furthermore, the ideal switch block output provides its respective current and voltage measurements.

In addition, the surge arrester available in MATLAB/Simulink library has a nonlinear V-I characteristic, for each column, which is represented, in Figure 3.5, by a combination of three exponential functions of the form:

$$\frac{V}{V_{ref}} = k_i \left(\frac{I}{I_{ref}}\right)^{\frac{1}{\alpha_i}} \tag{3.1}$$

Where k_i and α_i are default parameters given by the manufacturers.

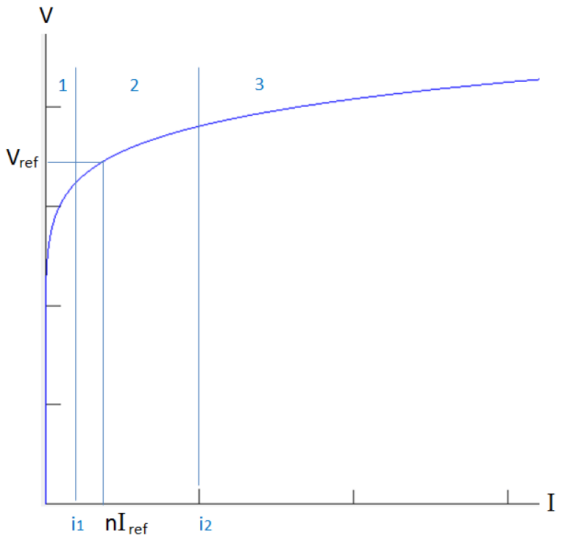

Figure 3.5: V-I characteristic of the surge arrester from MATLAB/Simulink

An ideal arrester must conduct electric current at a certain voltage above the rated voltage, hold the voltage with little change for the duration of overvoltage and substantially cease conduction at

very nearly the same voltage at which conduction started [28].

3.2 Mechanical DC Circuit Breaker

3.2.1 Modeling

To better comprehend the operation and fault clearance of a hybrid DC circuit breaker, it was necessary to simulate and analyse the behaviour of a mechanical DC circuit breaker.

The diagram of a mechanical DC circuit breaker, shown in Figure 3.6, created using MATLAB/Simulink presents the following parameters:

- DC Voltage: 400 kV;
- DC Current: 1200 A;
- L_{DC}: 0.1 H;
- Cable: 0.0095 Ω/km; L = 2.1 mH/km; C = 0.1906 μF/km;
- Resonant Circuit: L_r = 3 mH; C_r = 1 μF; R_r = 1200 Ω;
- Surge arrester: 600 kV;
- R_{load}: 330 Ω;
- Actuation time (control protection): 2.5 ms;

The DC voltage was decided accordingly to offshore wind farms studied during the state of the art and the DC current is in between the acceptable limits of the nominal current of the IGBT model chosen and mentioned above. The chosen resonant frequency was 2905 Hz, which allowed an opening time of 0.3(3) ms. The cable parameters correspond to a surge impedance of approximately 0.01 ohms.

In order to coordinate the opening and closing of the main and auxiliary circuit breakers, a state machine was implemented as figure 3.7 shows. As can be seen, a current protection level of 3 kA was chosen.

Furthermore, more diagrams were created, using MATLAB/Simulink, with the purpose of showing and comparing more compositions of a mechanical DC circuit breaker. Moreover, to analyse the possibility of a mechanical DC circuit breaker being used in a multi-terminal grid, a diagram with two source voltages was created.

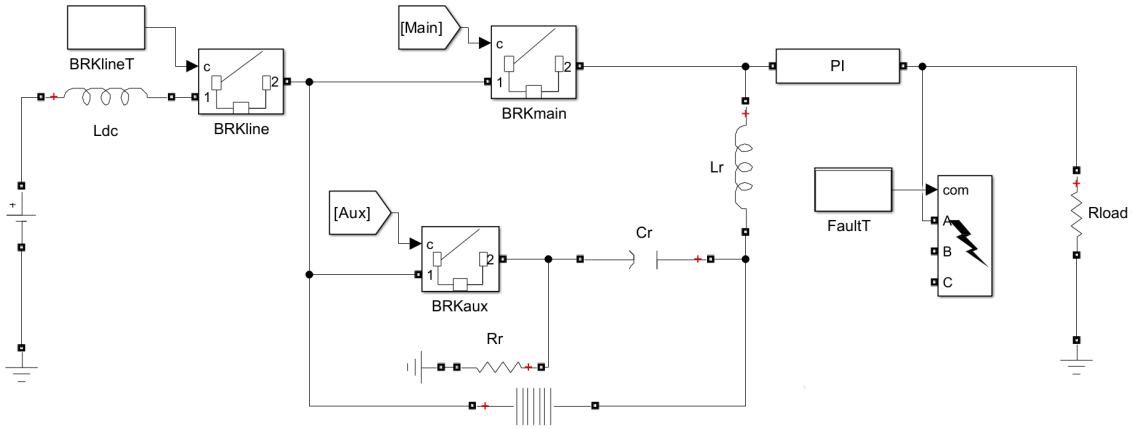

Figure 3.6: Mechanical DC circuit breaker built using MATLAB/Simulink.

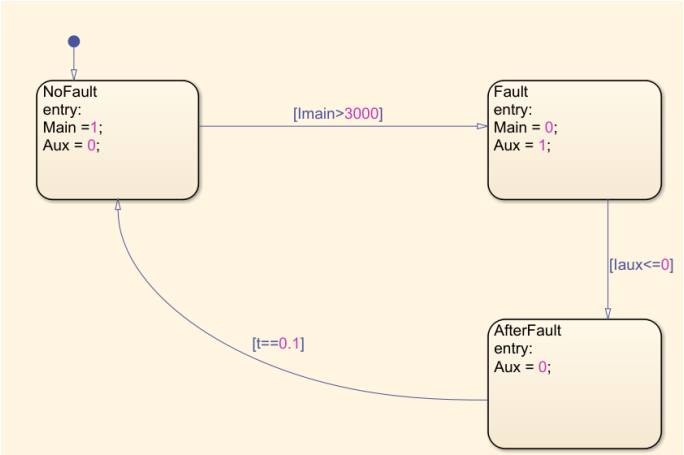

Figure 3.7: State machine used in the Mechanical DC circuit breaker simulation.

3.2.2 Case Studies and Results

Starting with the simulation of the diagram of Figure 3.6, which consists of a mechanical DC circuit breaker with the resonant circuit (L_r, C_r) placed on the right side of the auxiliary breaker (BRKaux).

A fault is applied at t = 0.02s and 10 km from the converter, while the grid protection is activated by the state machine, where the Fault state, that changes the state of the main breaker (BRKmain) from close to open (1 to 0) and the state of the auxiliary breaker from open to close (0 to 1), is reached when the main current (I_{main}) is higher than 3000 A. When the the BRKaux is fully closed, the resonant current is injected and, because the resonant circuit is on the right side of the breaker, is subtracted from the main current. The main current rapidly drops to zero and the Main breaker opens. When I_{aux} reaches 0 or is lower than 0 the state machine changes to the AfterFault state and the auxiliary breaker state changes from close to open (1 to 0).

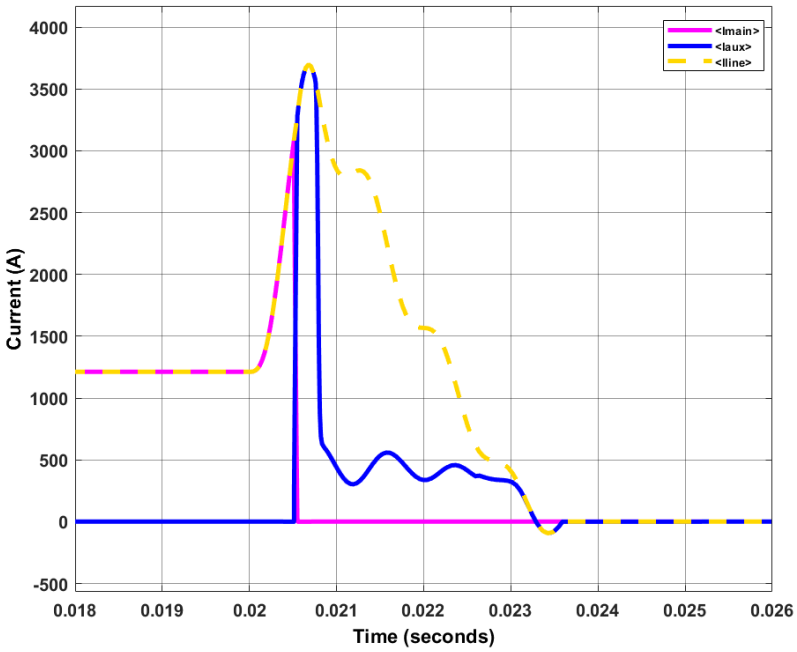

Figure 3.8: Current response (I_{main}, I_{aux}, I_{line}) to fault clearing.

Figure 3.8 shows that the fault is cleared in approximately 3.6 ms, which is also the opening time of the DC circuit breaker, and, as it was expected, when the auxiliary current starts to rise the main current starts to decrease. Additionally, figure 3.9 presents the voltage in the main breaker and in the arrester, which have a similar behaviour and stabilize, at the nominal voltage, 15 ms after the fault occurs. Finally, figure 3.10 shows the energy absorbed by the surge arrester during the fault clearance, which reaches around 1.7 MJ.

Another diagram of a mechanical DC breaker was built, however, the resonant circuit was placed on the left side of the auxiliary breaker, as figure 3.11 displays.

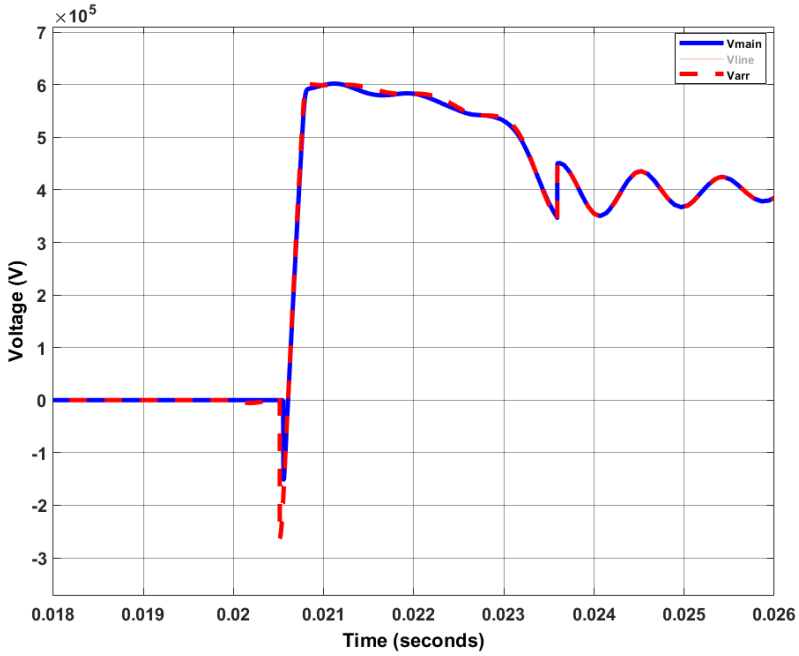

Figure 3.9: Main breaker and arrester's voltage during fault clearing.

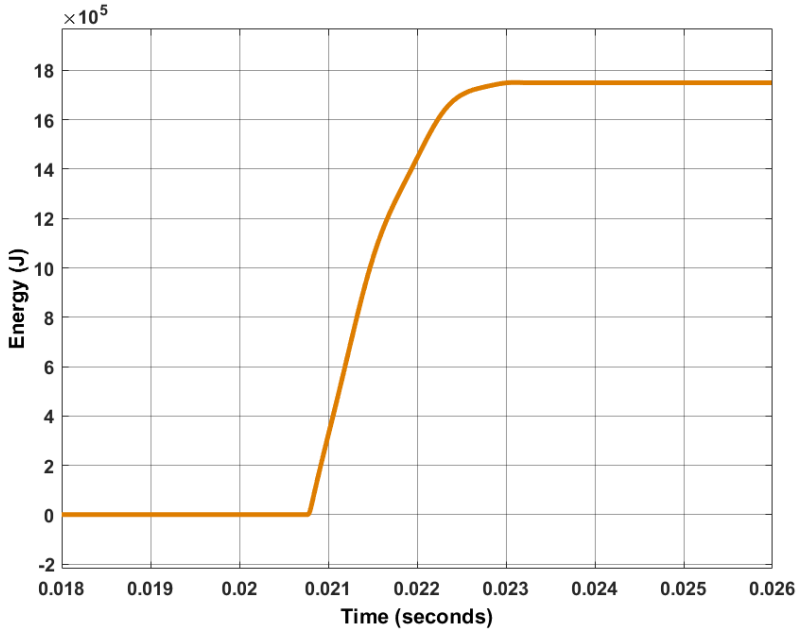

Figure 3.10: Energy absorbed by the surge arrester.

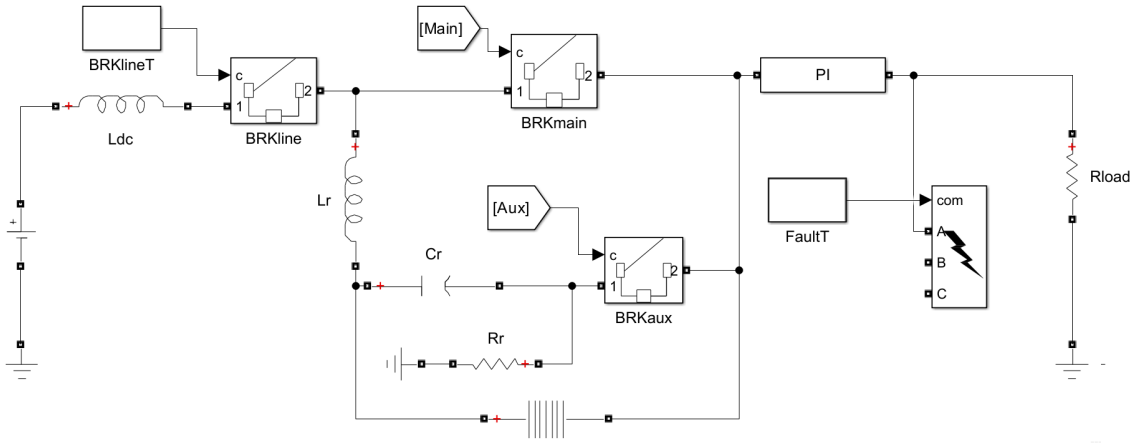

Figure 3.11: Mechanical DC circuit breaker, whith resonant circuit placed on the left of BRKaux

The difference between the two simulations mentioned above is that with the resonant circuit on the left side of the auxiliary breaker the resonant current is going to be added to the DC current as the results in figure 3.12 present. I_{main} increases and decreases with the increment and decrement of I_{aux}. Consequently, the clearing fault time expands, and it takes approximately 5 ms. However, the opening time decreases and it is about 1 ms.

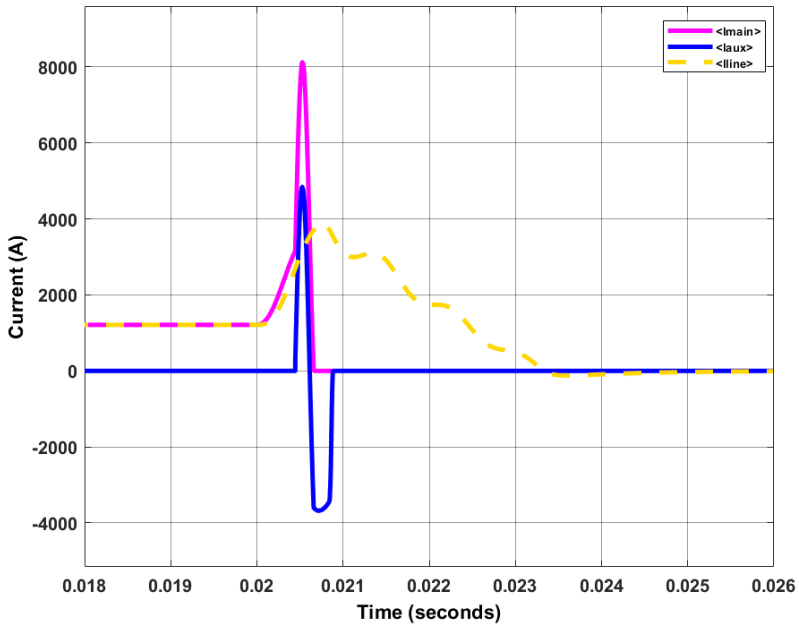

Figure 3.12: Current response (I_{main}, I_{aux}, I_{line}) to fault clearing.

The system voltages can be analysed in 3.13, where they stabilize 17 ms after the fault occurs. In addition, Figure 3.14 displays the amount of energy absorbed by the arrester, that reaches a maximum value of 2.6 MJ, double than the amount of energy absorbed in the previous case.

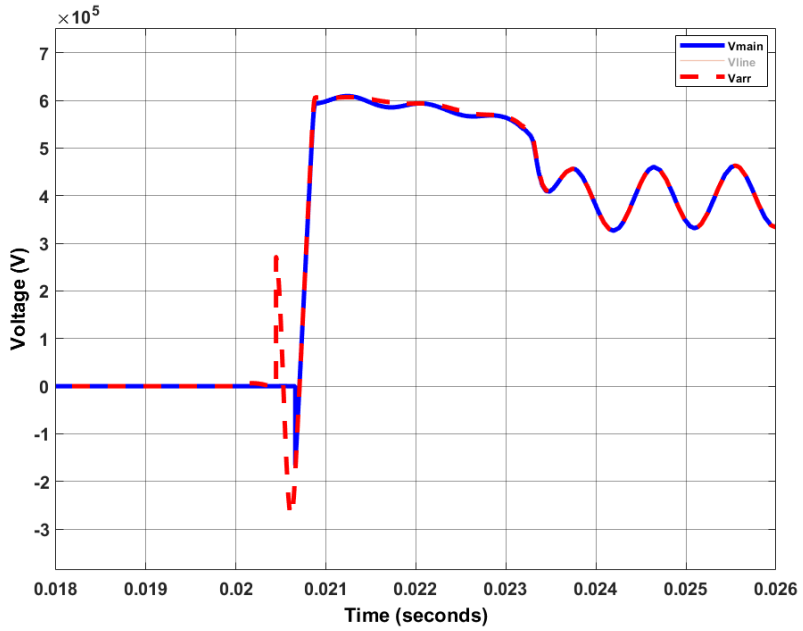

Figure 3.13: Main breaker and arrester's voltage during fault clearing.

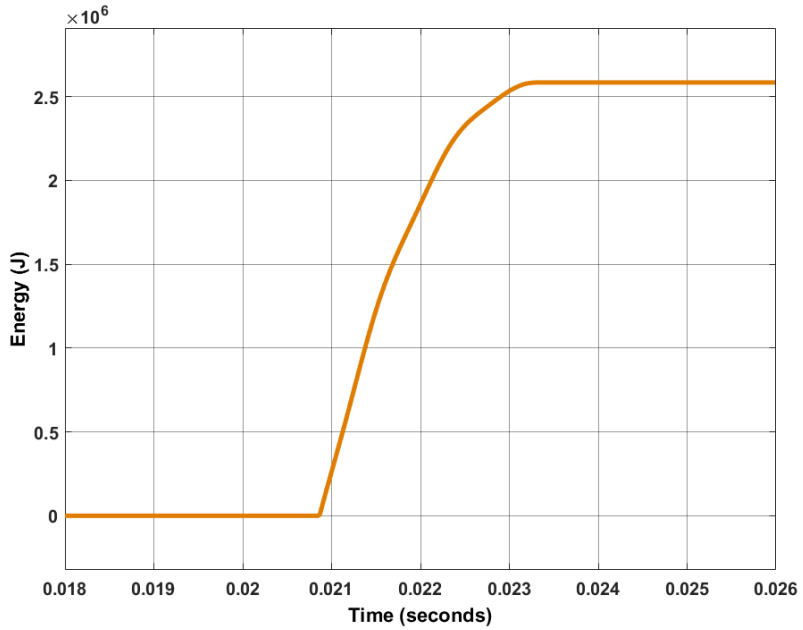

Figure 3.14: Energy absorbed by the surge arrester.

In order to study selectivity, a second mechanical DC circuit breaker was placed in series with an extra voltage source of 398.8 kV, as Figure 3.15 shows. Additionally, the mechanical DC circuit breaker on the left is 70 km from the fault, while the circuit breaker on the right is 30 km from the fault. These conditions allowed a DC current of 1200 A from the left to the right terminal.

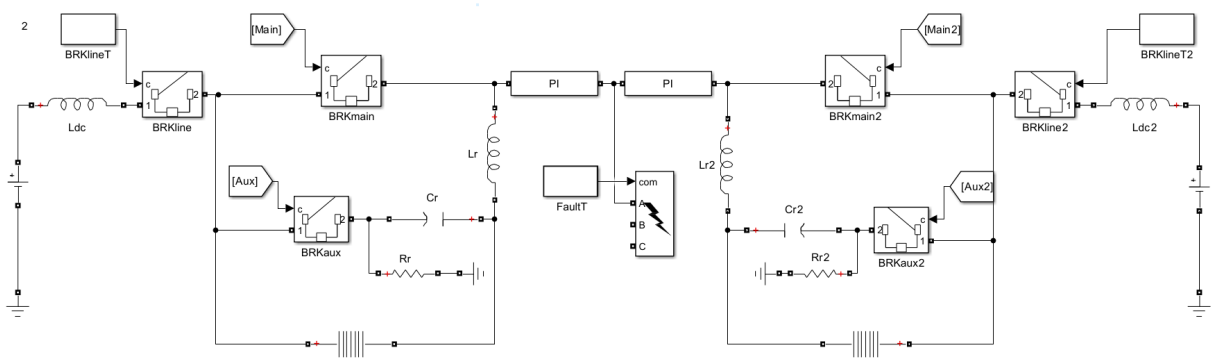

Figure 3.15: Two Mechanical DC circuit breaker in a system with 2 voltage sources.

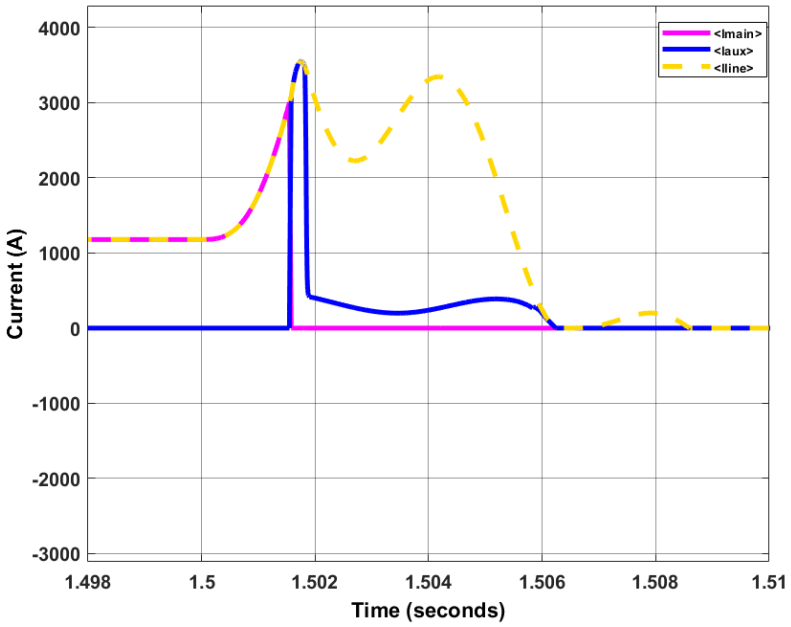

Figure 3.16: Current response (I_{main}, I_{aux}, I_{line}) to fault clearing.

A fault is applied at 1.5 s and, as Figures 3.16 and 3.17 present, the second DC circuit breaker clears the fault faster then the first circuit breaker, since it is closer to where the fault is applied. The DC circuit breaker on the left eliminates the fault at around 1.509 s, while the DC circuit breaker on the right clears the fault at approximately 1.505 s. The influence of the distance from the fault can also be observed in the arrester voltages of both DC circuit breakers. As Figures 3.18 and 3.19 demonstrate, the arrester's voltage stabilizes earlier on the right side of the system. Figures 3.20 and 3.21 demonstrate the energy absorbed on both arresters.

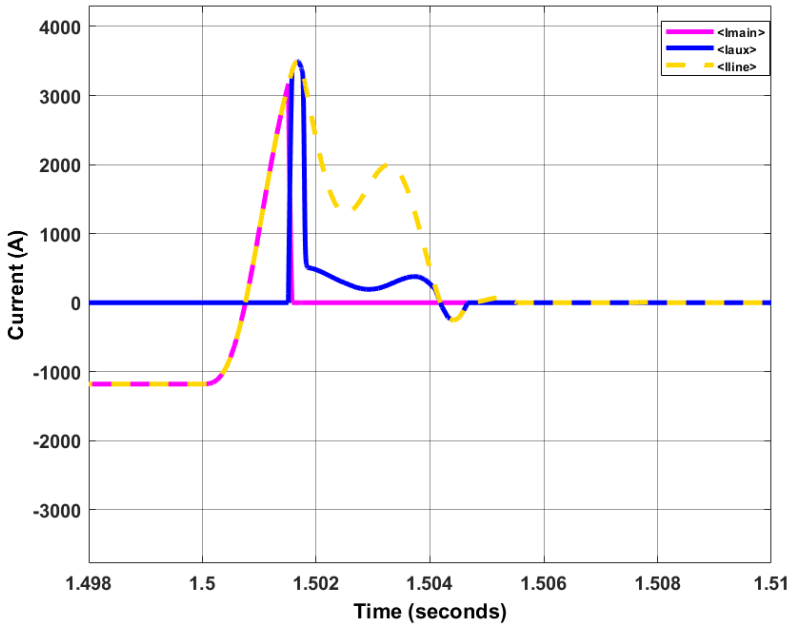

Figure 3.17: Current response (I_{main2}, I_{aux2}, I_{line2}) to fault clearing.

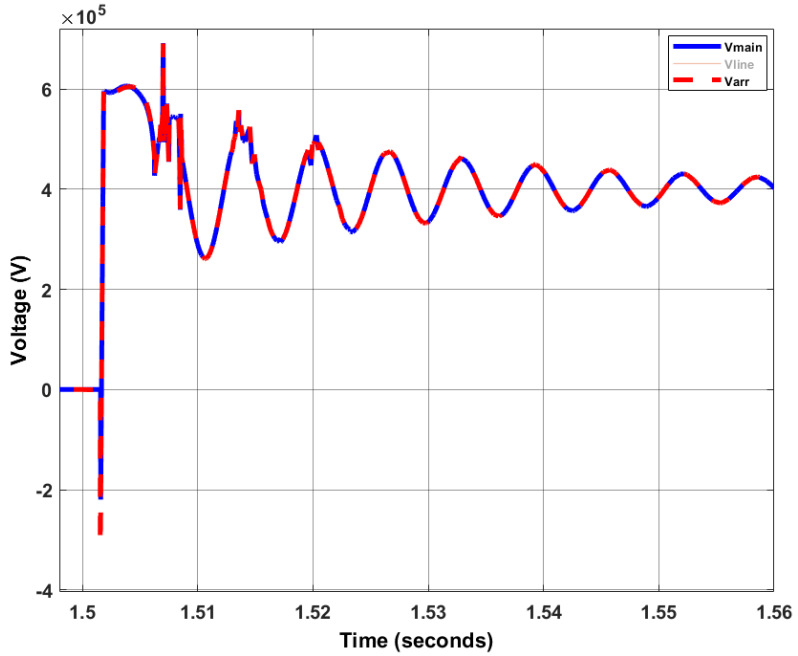

Figure 3.18: Main breaker and arrester's voltage during fault clearing.

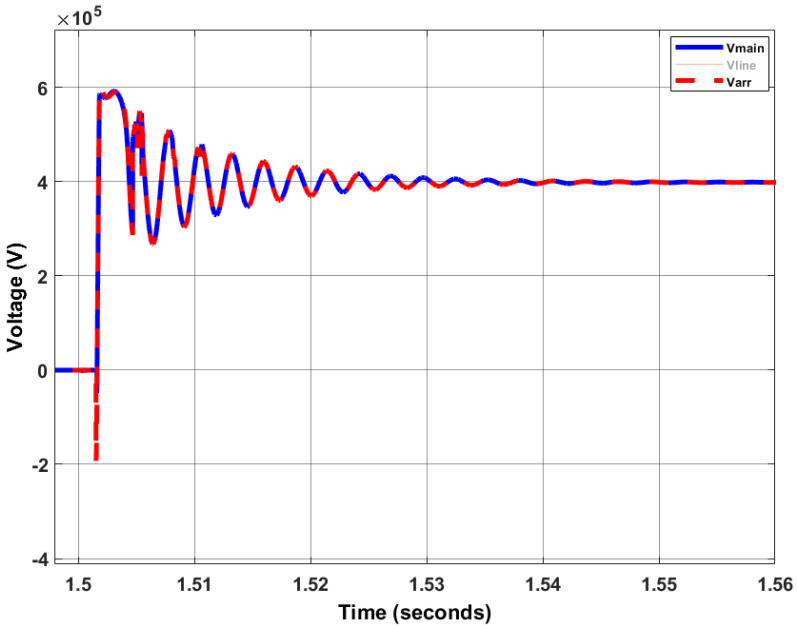

Figure 3.19: Main breaker 2 and arrester2's voltage during fault clearing.

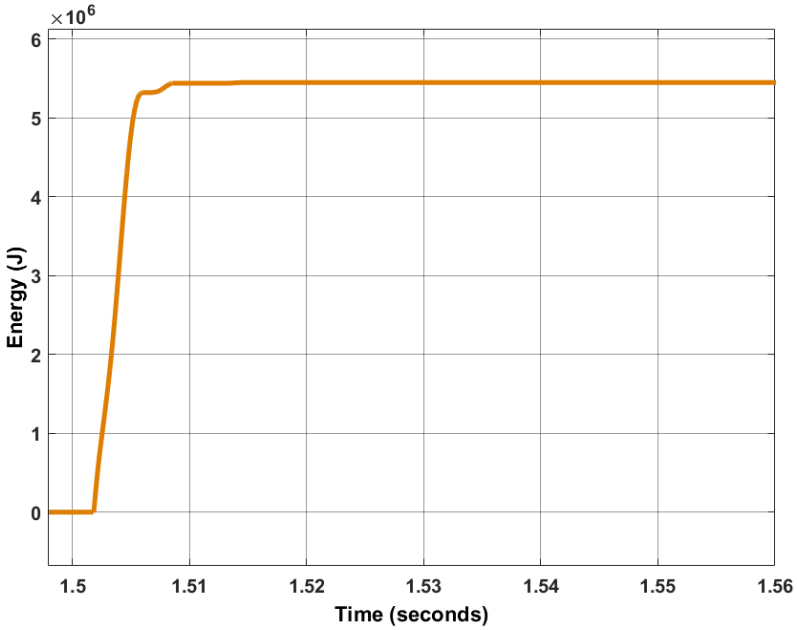

Figure 3.20: Energy absorbed by the the surge arrester

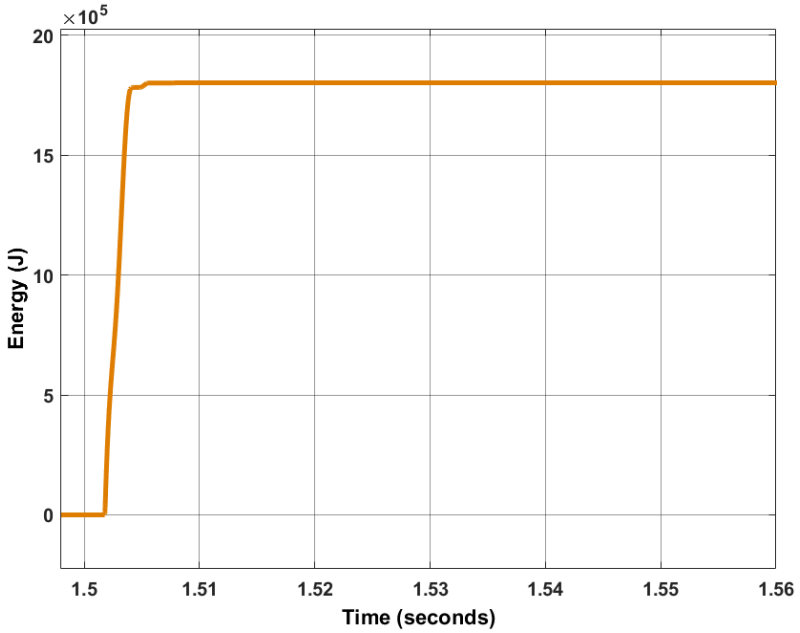

Figure 3.21: Energy absorbed by the the surge arrester2

3.3 Hybrid DC Circuit Breaker

3.3.1 Modeling

After the study of a mechanical DC circuit breaker, a diagram of a hybrid DC circuit breaker was modeled using MATLAB/Simulink, as Figure 3.22 shows. The parameters are identical to the parameters used in the modeling of the mechanical DC circuit breaker, with the exception of the resonant circuit, which does not exist, and with the addition of the internal resistance of the IGBTs.

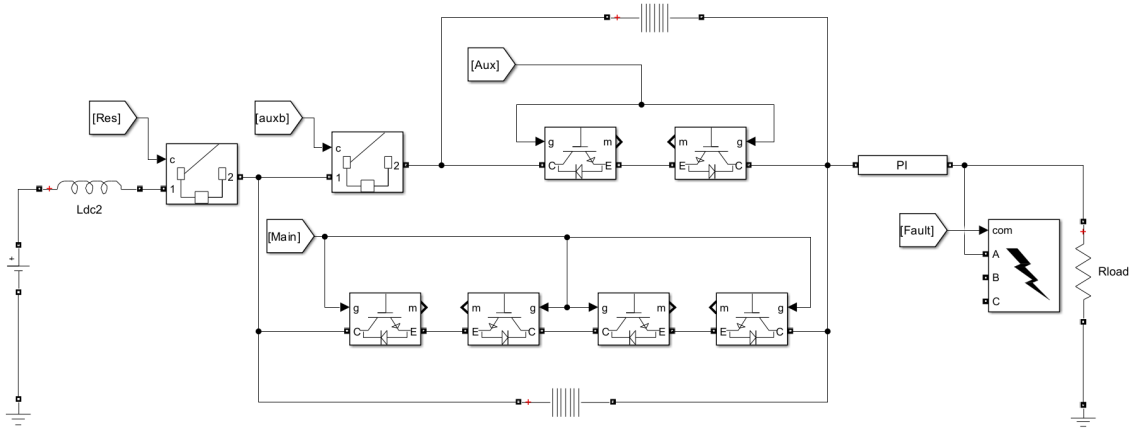

Figure 3.22: Hybrid DC circuit breaker.

The hybrid DC circuit breaker is composed by the main and the auxiliary breaker, as mentioned previously in chapter 2. The IGBTs of the auxiliary breaker have an internal resistance of 0.7 mΩ

and a constant voltage drop of 1.5 V. Moreover, the IGBTs of the main breaker have a total internal resistance of 140 mΩ and a total voltage drop of 300 V (it was considered a set of 200 switches in series). This different values between the internal resistance and voltage drop of the IGBTs allows the current to flow through the auxiliary breaking during normal operation.

In addition, a new state, Communication, was added to the prior state machine, as Figure 3.23 shows.

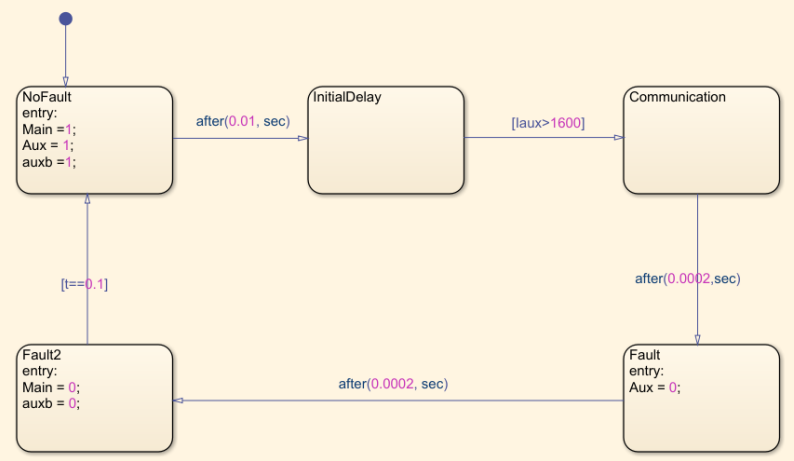

Figure 3.23: State machine used in the Hybrid DC circuit breaker simulation.

3.3.2 Case Studies and Results

A fault is applied at t = 0.02s and 10 km from the converter, while the grid protection is activated by the state machine, where the NoFault state maintains the main breaker, the auxiliary breaker and the circuit breaker (auxb) closed. When a fault occurs and I_{aux} exceeds 1600 A the state changes to Communication state. After 0.2 ms the state changes to Fault state, representing the time that the system takes to detect a fault and order the breaker to open. In Fault state only the auxiliary breaker opens (Aux = 0), allowing the current to commutate to the main breaker. Furthermore, after 0.2 ms the state changes to Fault2, where auxb and the main breaker open.

The evolution of the system currents is shown in Figure 3.24 and, although the fault is cleared after 10 ms, the hybrid circuit breaker opens in 0.6 ms. Similarly, the voltages across the main breaker and the surge arrester are represented in Figure 3.25. Finally, Figure 3.26 shows the energy absorbed by the surge arrester, which reaches 1.05 MJ.

In addition, in order to study the selectivity of the hybrid circuit breaker, a second one was added in series with a voltage source of 398.8 kV, as presented in figure 3.27. The fault is applied at t = 10 s and 30 km from the hybrid DC circuit breaker on the left and 70 km from the hybrid DC circuit breaker on the right.

In Figures 3.28 and 3.29 it is possible to observe that the hybrid circuit breaker on the left side of the fault, which is also the closest to it, clears the fault first, around 10.0045 s, while the right hybrid circuit breaker clears the fault approximately around 10.0065 s.

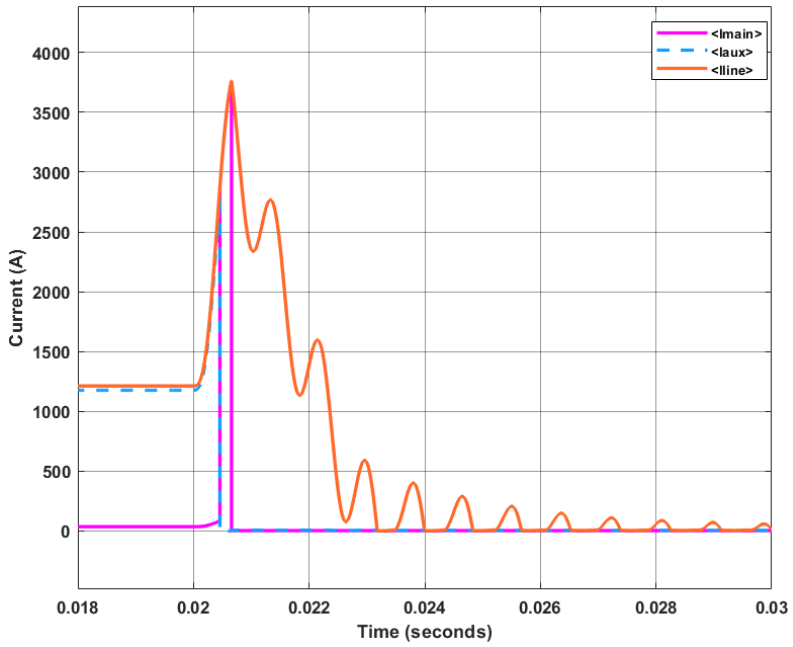

Figure 3.24: Current response (I_{main}, I_{aux}, I_{line}) to fault clearing.

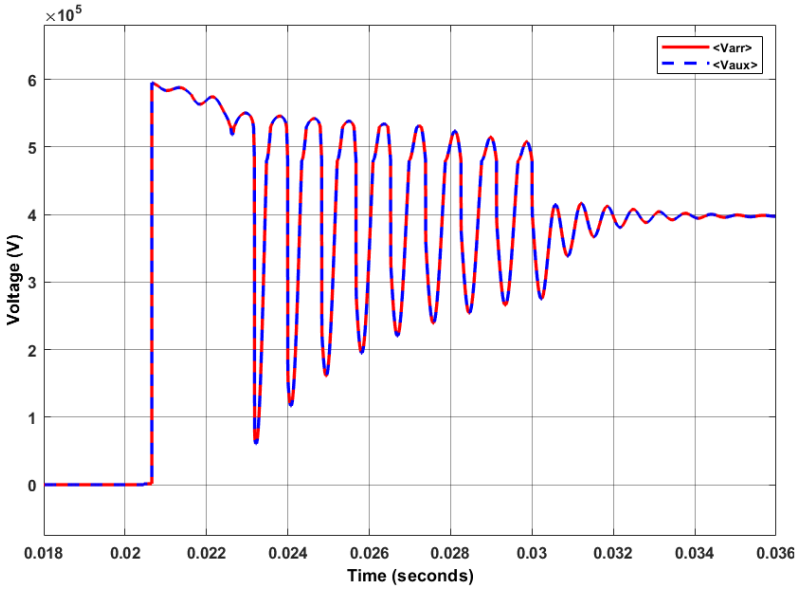

Figure 3.25: Main breaker and arrester's voltage during fault clearing.

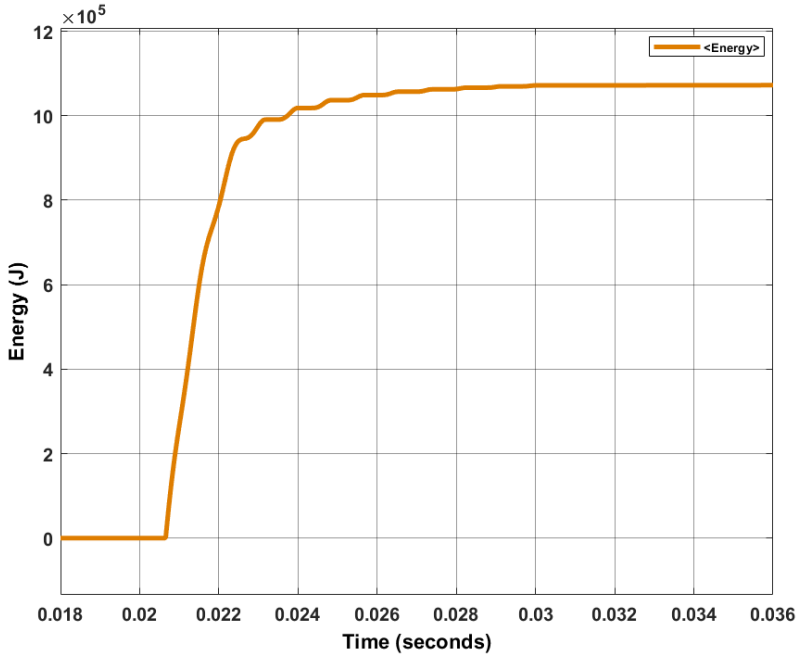

Figure 3.26: Energy absorbed by the surge arrester.

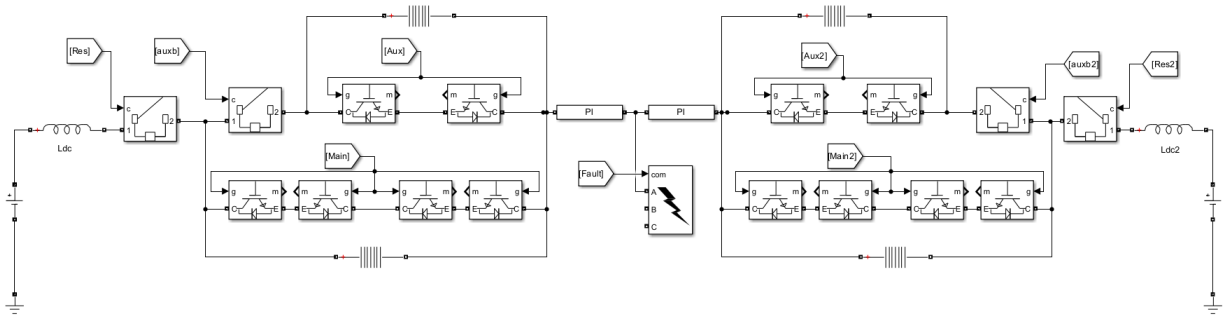

Figure 3.27: Two Hybrid DC circuit breakers in a system with 2 voltage sources.

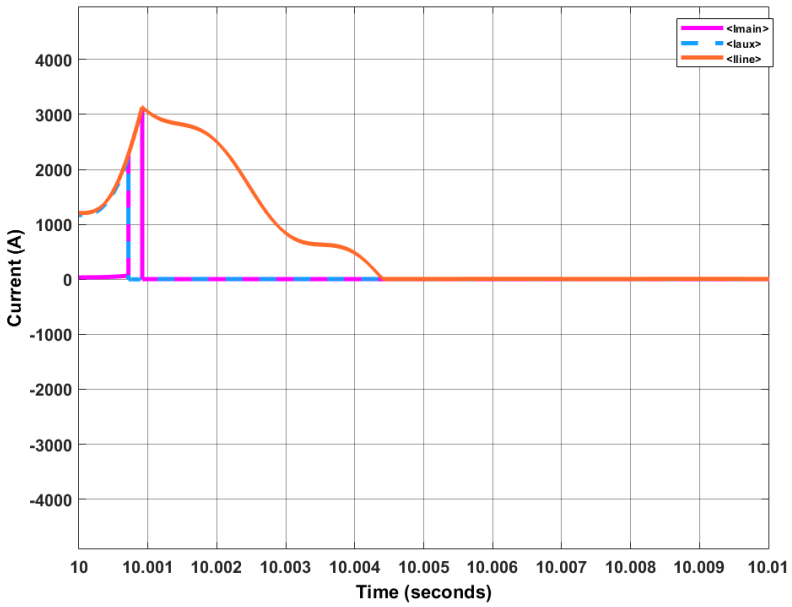

Figure 3.28: Current response (I_{main}, I_{aux}, I_{line}) to fault clearing.

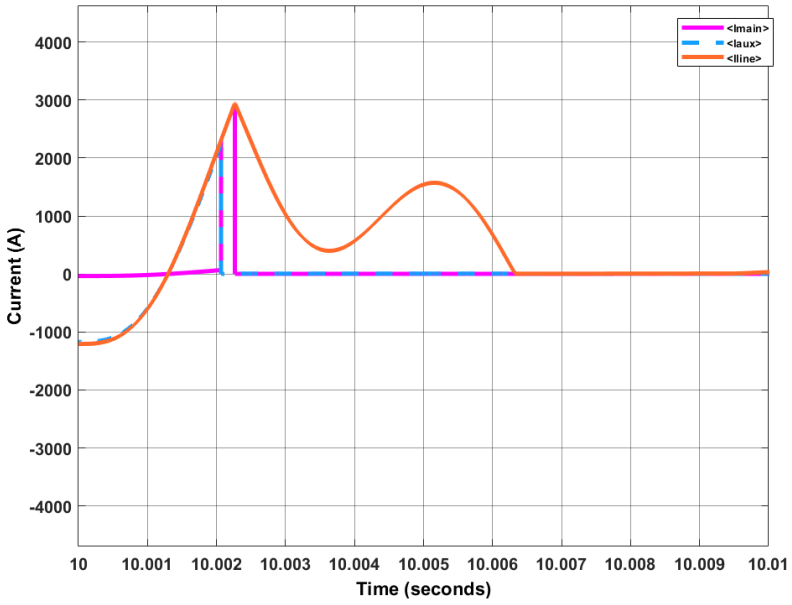

Figure 3.29: Current response (I_{main2}, I_{aux2}, I_{line2}) to fault clearing.

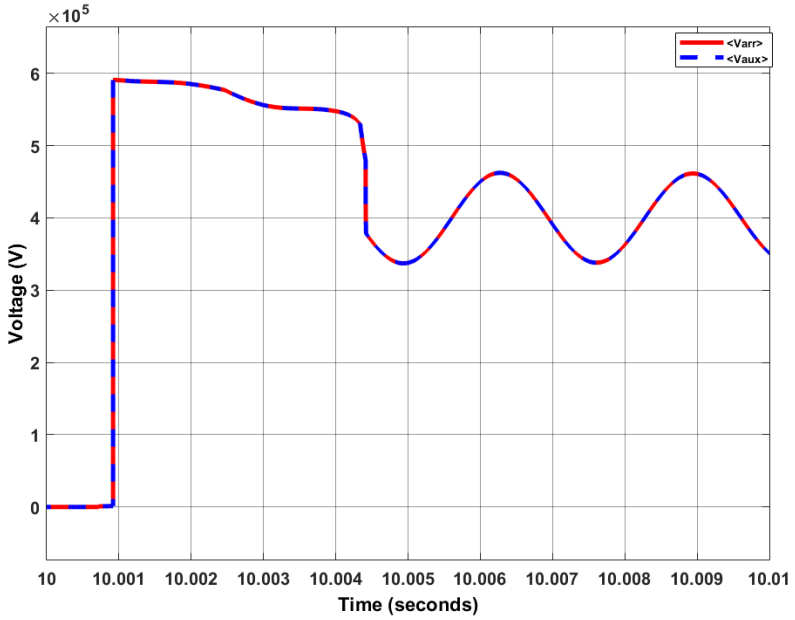

Figure 3.30: Main breaker and arrester's voltage during fault clearing.

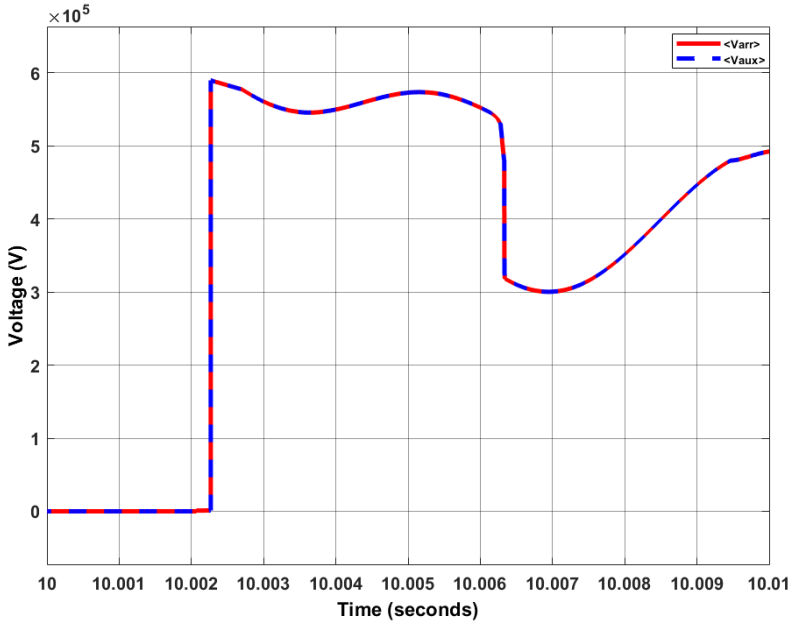

Figure 3.31: Main breaker 2 and arrester2's voltage during fault clearing.

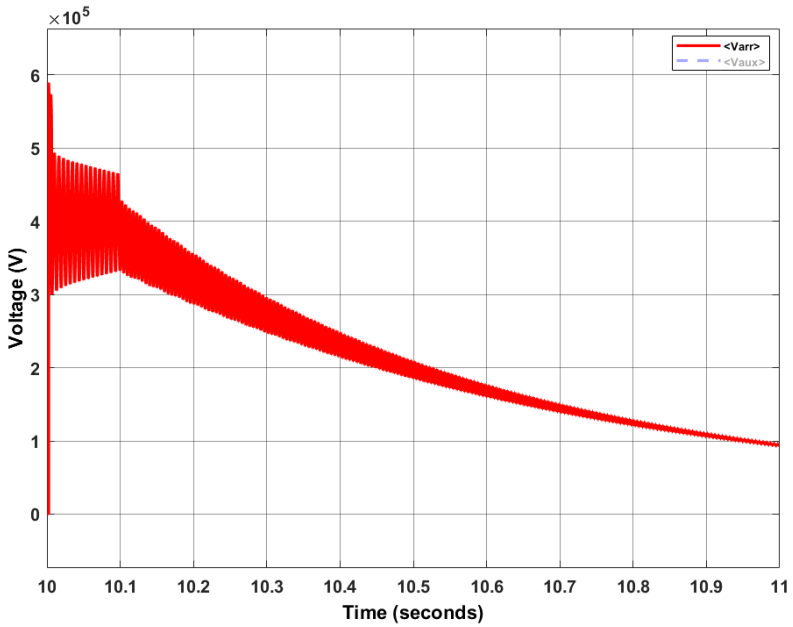

Figure 3.32: Voltage behaviour of arrester2 during fault clearing.

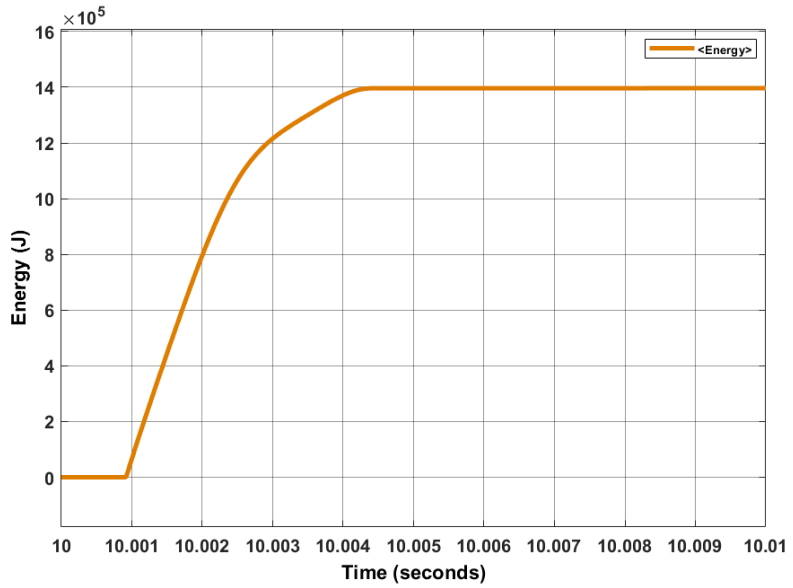

Figure 3.33: Energy absorbed by the the surge arrester

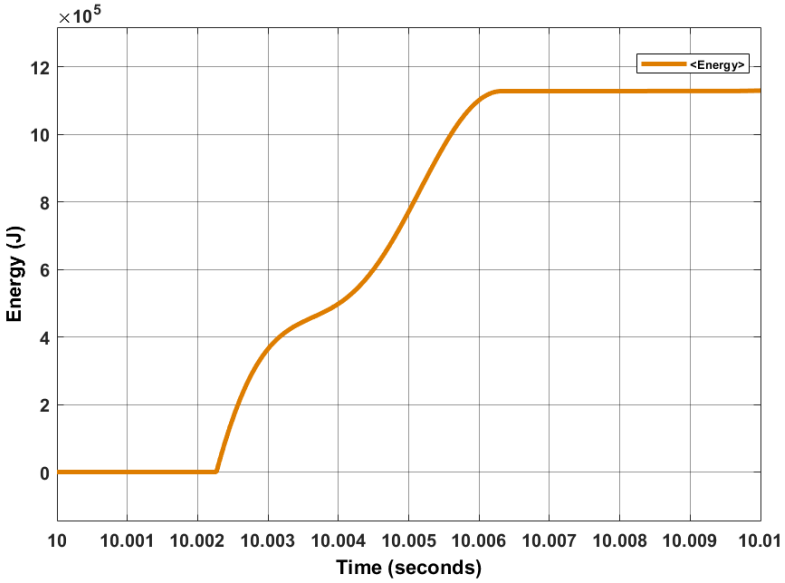

Figure 3.34: Energy absorbed by the the surge arrester2

It is also possible to analyze the main breakers and surge arresters voltages in Figures 3.30 and 3.31, which also indicate that the hybrid circuit breaker on the left actuates first, since the voltage peaks at 10.001 s while on the right circuit breaker the voltage peaks approximately 1.25 ms after.

Moreover, The voltage across arrester2 is shown again in Figure 3.32, in this case its evolution during the full fault clearing interval. Figures 3.33 and 3.34 show the energy absorbed by both surge arresters and, as expected, the absorbed energy by the right arrester is somewhat smaller than the one in the left side due to the faster decay of the current.

3.4 Discussion

In the two first case studies of the mechanical DC circuit breaker, by comparing the results, it is possible to conclude that placing the resonant circuit on the right side of the auxiliary breaker is more reasonable, because, although the opening time is higher, the currents reach values that can compromise the electronic devices and more energy has to be absorbed by the surge arrester.

Furthermore, when comparing the first case study of the mechanical DC circuit breaker with the first case study of the hybrid DC circuit breaker, even though both reach similar peak currents, it is clear that the hybrid DC circuit breaker has the fastest opening time (0.6 ms).

Additionally, by analysing the selectivity case studies with higher distances to the fault, it is possible to observe that both breakers have selectivity capacities, but the hybrid DC circuit breaker still has the smaller opening time.

Lastly, the surge arrester of the mechanical circuit breaker absorbs more energy in comparison with the hybrid circuit breaker.

For the reasons stated above, the hybrid circuit breaker is the most secure option.

Chapter 4

Conclusion and Future Work

4.1 Main Conclusions

In this dissertation it was studied that offshore wind farms at long distances from the coast use HVDC transmission cables. For this reason, the protection devices utilized are HVDC circuit breakers. Using MATLAB/Simulink, five models of systems with HVDC circuit breakers were implemented.

Firstly, two models of mechanical DC circuit breaker were created, one with the resonant circuit on the left of the auxiliary breaker and the other with the resonant circuit on the right. These models helped better understand the influence of the parameters of the resonant circuit in the current zero crossing, which is essential for a mechanical DC circuit breaker to work properly.

Secondly, a model with two mechanical DC circuit breakers and different distances to the fault were built, in order to better understand the selectivity of the circuit breaker. These mechanical circuit breaker studies facilitated the implementation of the following hybrid circuit breakers models.

Finally, a system with a hybrid circuit breaker was created and also a system to study its selectivity.

By comparing the results obtained to the results of the mechanical circuit breaker it was clear that to assure the protection of offshore wind farms with HVDC transmissions hybrid CBs appear to be the most plausible and effective solution, due to their reaction speed and insignificant losses. However, it is still necessary to continue to study hybrid CBs and their influence in HVDC transmission offshore, since the distance from the wind farms to the coast is growing and the need to generate more power is also increasing.

4.2 Future Work

The main goal of this dissertation was to demonstrate that hybrid circuit breakers are more suitable to use in a HVDC transmission, but there are some suggestions of case studies that can expand the

knowledge about hybrid circuit breakers such as improving the selectivity model, by creating an algorithm that allows only the closest circuit breaker to actuate.

Another interesting study should be to apply the previous model to a multi-terminal HVDC grid and analyze the behaviour of the circuit breaker.

It would be also interesting to try to build an experiment, with real electric elements but with reduced scale parameters.

References

[1] O. Anaya-Lara, D. Campos-Gaona, E. L. Moreno-Goytia, and G. P. Adam. *Offshore Wind Energy Generation: Control, Protection, and Integration to Electrical Systems*. John Wiley Sons, Ltd, West Sussex, UK, 2014.

[2] M. Parker, S. Finney, and D. Holliday. DC protection of a multi-terminal HVDC network featuring offshore wind farms. 9th International Conference on Applied Energy (ICAE), Cardiff, UK, 21-24 August 2017. doi: https://doi.org/10.1016/j.egypro.2017.12.588.

[3] D. Jovcic. *High Voltage Direct Current Transmission - Converters, Systems and* DC *Grids (2nd Edition)*. John Wiley & Sons, Ltd, West Sussex, UK, 2019.

[4] P. Breeze. *Wind Power Generation*. Elsevier Ltd., 2016. doi: https://doi.org/10.1016/C2014-0-04850-2.

[5] T. Ackermann and L. Soder. *Wind Power in Power Systems: An Introduction*, book section 4. John Wiley & Sons, Ltd, West Sussex, UK, 2012.

[6] S. M. Alagab, S. Tennakoon, and C. Gould. Review of wind farm power collection schemes. In *50th International Universities Power Engineering Conference (UPEC)*, Stoke on Trent, UK, 2015, pp. 1-5, doi: https://doi.org/10.1109/UPEC.2015.7339922.

[7] K. Das and N. A. Cutululis. Offshore wind power plant technology catalogue - components of wind power plants, AC collection systems and HVDC systems. Report, 2017.

[8] J. Qi, W. Zhao, and X. Bian. Comparative study of SVC and STATCOM reactive power compensation for prosumer microgrids with DFIG-based wind farm integration. *IEEE Access*, 8:209878–209885, 2020. doi: https://doi.org/10.1109/ACCESS.2020.3033058.

[9] B. Li and J. He. *Protection Principle and Technology of the VSC-Based DC Grid*. Springer Nature Singapore Pte Ltd., Singapore, 2020.

[10] M. Callavik, A. Blomberg, J. Häfner, and B. Jacobson. "The hybrid HVDC breaker: An innovation breakthrough enabling reliable HVDC grids", ABB grid systems. pages 1–10, November 2012.

[11] S. Wang, C. Li, O. D. Adeuyi, G. Li, C. E. Ugalde-Loo, and J. Liang. Coordination of MMCs with hybrid DC circuit breakers for HVDC grid protection. *IEEE Transactions on Power Delivery*, 34:11–22, 2019. doi: https://doi.org/10.1109/TPWRD.2018.2828705.

[12] D. Jovcic, T. Guangfu, and P. Hui. Adopting circuit breakers for high-voltage DC networks: Appropriating the vast advantages of DC transmission grids. *IEEE Power and Energy Magazine*, 17(3):82–93, 2019. doi: https://doi.org/10.1109/MPE.2019.2897408.

[13] J. Liang, O. Gomis-Bellmunt, and D. V. Hertem. *HVDC GRIDS: For Offshore and Supergrid of the Future*, pages 171–192. John Wiley & Sons, Inc., Hoboken, New Jersey, 2016.

[14] M. Barnes, D. S. Vilchis-Rodriguez, X. Pei, R. Shuttleworth, O. Cwikowski, and A. C. Smith. HVDC Circuit Breakers – A review. *IEEE Access*, 8:211829–211848, 2020. doi: https://doi.org/10.1109/ACCESS.2020.3039921.

[15] M. Hadjikypris and V. Terzija. Transient fault studies in a multi-terminal VSC-HVDC grid utilizing protection means through DC circuit breakers. In *2013 IEEE Grenoble Conference*, pages 1–6. doi: https://doi.org/10.1109/PTC.2013.6652480.

[16] R. D. Garzon. *High Voltage Circuit Breakers: Design and Applications*. MARCEL DEKKER, INC., 270 Madison Avenue, New York, New York 10016, 1997.

[17] J.B. Curis, J. Descloux, N. Grise, A. Wagner, Ö. Göksu, O. Saborío-Romano, C. Brantl, M. Kaiser, M. Quester, P. Ruffing, B. Dupont, P. Henneaux, K. Karoui, D. Nesterov, I. A. Irazabal, C. MacIver, and K Bell. Synthesis of available studies on offshore meshed HVDC grids. Report 1.3, Tractebel Engineering S.A, 2016.

[18] S. Liu, Z. Liu, J. J. Chavez, and M. Popov. Mechanical DC circuit breaker model for real time simulations. *International Journal of Electrical Power & Energy Systems*, 107:110–119, 2019. doi: https://doi.org/10.1016/j.ijepes.2018.11.014.

[19] *Network Protection Automation Guide: Protective Relays, Measurement Control*. Alstom Grid, 2011.

[20] J.C.Das. *Substation Automation and Communication Protocols Including* IEC *61850*, volume 4 of *Power Systems Handbook*, book section 16, pages 621–640. Power System Studies, Inc., Snellville, Georgia, USA, 2018.

[21] K. S. Nimma and F. S. Nimma. Modeling intelligent control switch IEC 61850 based substation automation communication. *Applied System Innovation*, 1(2):7, 2018. doi: https://doi.org/10.3390/asi1010007.

[22] A. A. Elbaset, Y. S. Mohamed, and A. N. A. Elghaffar. IEC 61850 communication protocol with the protection and control numerical relays for optimum substation automation system. *Engineering Science and Technology Review*, 13:1–12, 2019. doi: https://doi.org/10.25103/jestr.132.01.

[23] D. Bösche, E. D. Wilkening, H. Köpf, and M. Kurrat. Hybrid DC circuit breaker feasibility study. *IEEE Transactions on Components, Packaging and Manufacturing Technology*, 7(3):354–362, 2017. doi: https://doi.org/10.1109/TCPMT.2016.2613579.

[24] S. Liu and M. Popov. Development of HVDC system-level mechanical circuit breaker model. *International Journal Electrical Power and Energy Systems*, 103:159–167, 2018. doi: https://doi.org/10.1016/j.ijepes.2018.05.017.

[25] F. Mohammadi, K. Rouzbehi, M. Hajian, K. Niayesh, G. B. Gharehpetian, H. Saad, Mohd. Hasan Ali, and V. K. Sood. HVDC circuit breakers: A comprehensive review. *IEEE Transactions on Power Electronics*, 36(12):13726–13739, 2021. doi: https://doi.org/10.1109/TPEL.2021.3073895.

[26] A. Mokhberdoran, D. Van Hertem, N. Silva, H. Leite, and A. Carvalho. Multiport hybrid HVDC circuit breaker. *IEEE Transactions on Industrial Electronics*, 65(1):309–320, 2018. doi: https://doi.org/10.1109/TIE.2017.2719608.

[27] R. Smeets, L. van der Sluis, M. Kapetanovic, D. F. Peelo, and A. Janssen. *Switching In Electrical Transmission And Distribution Systems*. John Wiley & Sons, Ltd, West Sussex, UK, 2015.

[28] C. A. Christodoulou, F. A. Assimakopoulou, Ioannis F. Gonos, and I. A. Stathopulos. Simulation of metal oxide surge arresters behavior. In *2008 IEEE Power Electronics Specialists Conference*, pages 1862–1866, 2008. doi: https://doi.org/10.1109/PESC.2008.4592215.